R.P.I. Progress Report MP-3

A Progress Report for
July 1, 1968 to December 31, 1968

ANALYSIS AND DESIGN OF A CAPSULE LANDING SYSTEM AND SURFACE VEHICLE CONTROL SYSTEM FOR MARS EXPLORATION

NATIONAL AERONAUTICS AND SPACE
ADMINISTRATION

Grant NGL-33-018-091

Submitted by the Special Projects Committee

D.K. Frederick
P.K. Lashmet
G.N. Sandor
C.N. Shen
E.J. Smith
S.W. Yerazunis

February 15, 1969

School of Engineering

Rensselaer Polytechnic Institute

ABSTRACT

Investigation of problems related to the landing and controlling of a mobile planetary vehicle according to a systematic plan of exploration of Mars has been undertaken. Problem areas receiving consideration include: updating of atmosphere parameters during entry, adaptive trajectory control, unpowered aerodynamic landing, terrain modeling and obstacle sensing, vehicle dynamics and attitude control, and chromatographic systems design concepts. The specific tasks which have been undertaken are defined and the progress which has been made during the interval July 1, 1968 to December 31, 1968 is summarized. Projections for work to be undertaken during the next six months period are included.

TABLE OF CONTENTS

Analysis and Design of a Capsule Landing System and Surface Vehicle Control System for Mars Exploration

I. Introduction

The planned exploration of the planet Mars in the 1970's involves the landing of an excursion module on the martian surface. Following a successful landing, the exploration of the martian surface would be promoted considerably if the excursion model is mobile and if its motion can be controlled according to a specific plan of exploration. Contributing to the formidable problems to be faced by such a mission are the existence of an atmosphere whose parameters are at this time rather uncertain within broad limits and the information transmission delay time between Martian and Earth control units. With the support of NASA Grant NGL-33-018-091, a number of important problems originating with the factors noted above have been investigated by a faculty-student team at Rensselaer.

The problems under study fall into two broad categories: (a) capsule landing and (b) control of a mobile exploration unit, from which a considerable number of specific tasks have been defined. This progress report describes the tasks which have been undertaken and documents the progress which has been achieved in the interval July 1, 1968 to December 31, 1968 and projects activity for the next period ending June 30, 1969.

II. Definition of Tasks

The uncertainty in martian atmosphere parameters and the delay time (order of ten minutes) in round trip communication between Mars and Earth underlie unique problems relevant to martian and/or other planetary explorations. All phases of the mission from landing the capsule in the neighborhood of a desired position to the systematic traversing of the surface and the attendant detection, measurement, and analytical operations must be consummated with a minimum of control and instruction by earth based units. The delay time requires that on board systems capable of making rational decisions be developed and that suitable precautions be taken against potential catastrophic failures such as vehicle flipover. Five major task areas, which are in turn divided into appropriate sub-tasks, have been defined and are listed below.

A. Trajectory Control

A.1. Martian Atmosphere Updating - Uncertainty in martian atmosphere parameters preclude _a priori_ trajectory and landing specifications. The objective of this task is to develop methods for updating martian atmosphere parameters on the basis of measurements obtained during entry. The updated parameters will be used by an adaptive trajectory control system, Task A.2., and during unpowered aerodynamic landing, Task B.

A.2. Adaptive Trajectory Control - If updated martian atmosphere parameters can be obtained during entry, an adaptive trajectory control system can be used to achieve the desired velocity, range and altitude parameters prior to the final landing phase. This task is concerned with methods by which to achieve the desired terminal conditions given the availability of updated atmospheric parameters.

B. Unpowered Aerodynamic Landing. The existence of an atmosphere on Mars, slight as it is, offers an opportunity for unpowered landing of the capsule through the use of aerodynamic forces. The objective of this task is to investigate the feasibility of devices utilizing aerodynamic forces to effect an acceptable landing approach and touchdown.

C. Surface Navigation and Path Control. Once the capsule is landed and the roving vehicle is in an operational state, it is necessary that the vehicle can be directed to proceed under remote control from the landing site to specified positions on the martian surface. This task is concerned with the problems of terrain modeling, path selection and navigation between the initial and terminal sites when major terrain features precluding direct paths are to be anticipated. On board decision making capability must be designed to minimize earth control responsibility except in the most adverse circumstances.

C.1. Terrain Sensing - The problem of gross navigation and path selection, requires major terrain feature information. The objective of this task is to define a system which will provide the required information describing the surrounding terrain to permit path selection decisions to be made.

C.2. Short Range Obstacle Sensing and Avoidance - It can be expected that many minor obstacles will be encountered by a roving vehicle. The objective of this task is to investigate and define methods of short range obstacle detection to provide the information necessary for steering and maneuvering control components to avoid such obstacles and to allow the gross navigation plan to be implemented.

D. Vehicle Dynamics and Attitude Detection Systems.

D.1. Vehicle Dynamics - As the vehicle negotiates the martian surface according to periodic instructions from Earth, it will encounter an uncertain terrain. Depending on the apparatus, instruments and devices with which the vehicle is equipped to meet mission objectives, particular requirements as to vehicle reaction, i.e., forces, orientation, etc., to the terrain may have to be satisfied. In addition, the response of the vehicle to potential terrain features of appropriate scale and repetitious nature must not be unacceptable. The objective of this task is to establish vehicle parameters, i.e., dimensions, arrangements, suspension details, satisfying mission requirements.

D.2. Attitude Detection Systems - Effective attitude detection systems will be required not only while the vehicle is stationary to permit planned experimentation to be undertaken and to make essential terrain measurements but also when the vehicle is in motion to provide information for the effective interpretation of obstacle detector signals and to provide alarms if the slope of the local terrain approaches critical values.

E. Chemical Analysis of Specimens. A major objective of martian surface exploration will be to obtain chemical, biochemical or biological information. Most experiments proposed for the mission require a general duty, chromatographic separator prior to chemical analysis by some device. The objective of this task is to generate fundamental data and concepts required to optimize such a chromatographic separator according to the anticipated mission.

The tasks defined above have been pursued by a team of six faculty members and twenty students. Of this group of students, ten have or will be receiving some financial support from the project while the remainder are participating without remuneration in order to fulfill their academic requirement of engineering project. Details of the student team including their degree objective, support relationship and period of participation are given in Section IV. Section III which follows summarizes the progress which has been made during the prior period and projects activities for the coming period, January 1 to June 30, 1969.

III. Summary of Results

Task A. Trajectory Control

The control of trajectory prior to the final landing phase involves two major problem areas both of which originate with the present uncertainties of the parameters of the martian atmosphere. The first of these areas is concerned with the development of methods by which to update the atmosphere parameters during entry and an assessment of the implications of measurement errors. The second of these areas is related to trajectory control in terms of terminal velocity using thrust or drag devices to permit for a proper transition into the final landing phase.

Task A.1.a. On-Line Updating of the Martian Atmosphere with Minimum Storage - R.E. Janosko
Faculty Advisor: Prof. C.N. Shen

This task is concerned with the problem of updating parameter estimates for the martian atmosphere during descent to provide data required for an effective control of trajectory, Ref. 1. In brief, measurements of the density of the atmosphere made at appropriate intervals are to be used to determine the parameters of the martian atmosphere assuming that the standard adiabatic density model applies throughout the whole atmosphere, Ref. 2. Task A.1.b. is concerned with the applicability of this parameter updating system to that section of the atmosphere above the tropopause which known to follow the exponential rather than the adiabatic model.

The practical problem of updating the adiabatic model parameters is extremely sensitive to the allowances made for measurement errors. Previous work, Ref. 3, had been concerned with methods for updating parameters assuming negligible measurement error. Summarized below is the progress achieved to date given that measurements involve uncertainty. Details of the updating systems and their implications are provided in Ref. 2 which is a detailed technical report on this phase of the project.

In dealing with the problem of updating the parameters given some measurement error, the standard adiabatic density equation, Ref. 4, is transformed to

$$\ln \rho = a_1 + a_2 \ln\left(\frac{1}{N} + a_3(1-x)\right) \tag{1}$$

where ρ is the mass density, and a_1, a_2 and a_3 are the parameters of interest. It is desired to determine and to continually update estimates of the parameters given measurements of density as a function of height.

Given a function of the form

$$y_n = fn\ (x_n, a_1, a_2, a_3) \tag{2}$$

it is desired to determine a_1, a_2, and a_3 from a set of data of the form

$$Y_n = F_n\ (x_n) \tag{3}$$

where in this case the y_n and Y_n correspond to the natural logarithm of the actual and measured density respeccively.

Two methods based on least squares approach are used to solve the problem applying concepts originally introduced by Levenberg, Ref. 5, and Hartley, Ref. 6.

First define the function

$$S(a_1, a_2, a_3) = \sum_{n=1}^{K} \left\{ W_n \left[-Y_i + F(x_n, a_1, a_2, a_3) + \frac{\partial f_n}{\partial a_1} \Delta a_1 + \frac{\partial f_n}{\partial a_2} \Delta a_2 + \frac{\partial f_n}{\partial a_3} \Delta a_3 \right] \right\}^2 \tag{4}$$

where the a_1, a_2, a_3 are estimates of the parameter values, the Δa_1, Δa_2, Δa_3 are the differences between the true and estimated parameter values, and the w_n is a statistical weighting factor applied to each data point which is set equal to one in the present analysis. $S(a_1,a_2,a_3)$ corresponds to a first order Taylor series expansion of the standard least-squares formula. This expansion is necessary because of the non-linearity of $F(x_n,a_1,a_2,a_3)$. One cannot solve directly for the true parameters a_1,a_2,a_3 but with equation (4) the problem is so formulated so as to allow for the solution of the difference between the estimated parameters and the true parameters.

Now minimize the function

$$J(a_1,a_2,a_3)=S(a_1,a_2,a_3)+\alpha_1(\Delta a_1)^2+\alpha_2(\Delta a_2)^2+\alpha_3(\Delta a_3)^2 \quad (5)$$

instead of the standard least square function. The α_1, α_2, α_3 are positive weights expressing the relative importance of minimizing each parameter value as well as indicating the relative value of minimizing the parameter changes versus the sum of the squares. It can now be assured that the parameter changes are small so that standard techniques can be used to solve for the minimum of Equation (5). By these techniques is obtained an equation of the form

$$\psi \underline{\Delta a} = \underline{\theta}$$

where
$$\{\psi_{ij}\} = \sum_{n=1}^{K} \left(\frac{\partial f_n}{\partial a_i}\right)\left(\frac{\partial f_n}{\partial a_j}\right), \quad i \neq j$$

$$= \sum_{n=1}^{K} \left(\frac{\partial f_n}{\partial a_i}\right)^2 + \alpha_i, \quad i \neq j \qquad (6)$$

$$\underline{\Delta a} = [\Delta a_1, \Delta a_2, \Delta a_3]^T$$

$$\underline{\theta} = [\theta_1, \theta_2, \theta_3]^T$$

$$\theta_i = \sum_{n=1}^{K} (F_n - f_n)\frac{\partial f_n}{\partial a_i} \quad i = 1,2,3$$

It should be noted that ψ is a 3x3 matrix, while $\underline{\Delta a}$ and $\underline{\theta}$ are column vectors.

Once the quantities Δa_i are determined, they are tested to see if the sum of the squares is minimized for the total incremental change or a fraction of it. The sum of the squares is calculated with zero, one half and the total parameter changes found. A parabola is then fitted to the three points and the minimizing increment of parameter change is found. The parameter changes are then given weights, $v_{i(opt)}$, corresponding to the weights which minimized the sum of the squares. The new estimates are then found from Ref. 6,

$$\tilde{a}_{i\ new} = \tilde{a}_{i\ old} + v_{i\ opt}\,\Delta a_i, 0 \leq v_i \leq 1 \qquad (7)$$

Since this overall scheme is computed once during each measurement interval, computational requirements are minimized.

Numerical testing of the above scheme indicates that it can properly update the parameters. Testing was for an assumed actual atmosphere corresponding to the VM-4 (10 mb surface pressure) model and an initial atmosphere estimated to correspond to the VM-8 (5mb surface pressure) model, Ref. 1.

Shown in Figure 1 is the effect of changing the relative weights of the sum of the squares with zero measurement error in the case where:

a_i^* = true value

a_i^o = initial estimate

$a_1^* = -9.907495 \qquad a_1^o = -10.572918$

$a_2^* = 2.325581 \qquad a_2^o = 2.702702$

$a_3^* = -.543916 \qquad a_3^o = 0.50155$

It should be noted that the weights suggested by Levenberg causes the parameter to diverge.

Figure 2 shows the effect of varying the relative weights among the parameters when random measurement errors with a standard deviation of .001 were simulated by Monte Carlo technique. Levenberg suggests equal α_i, yet this doesn't give the best result. By assigning appropriate weighting factors, smaller rms errors can be achieved in a very small number of iterations.

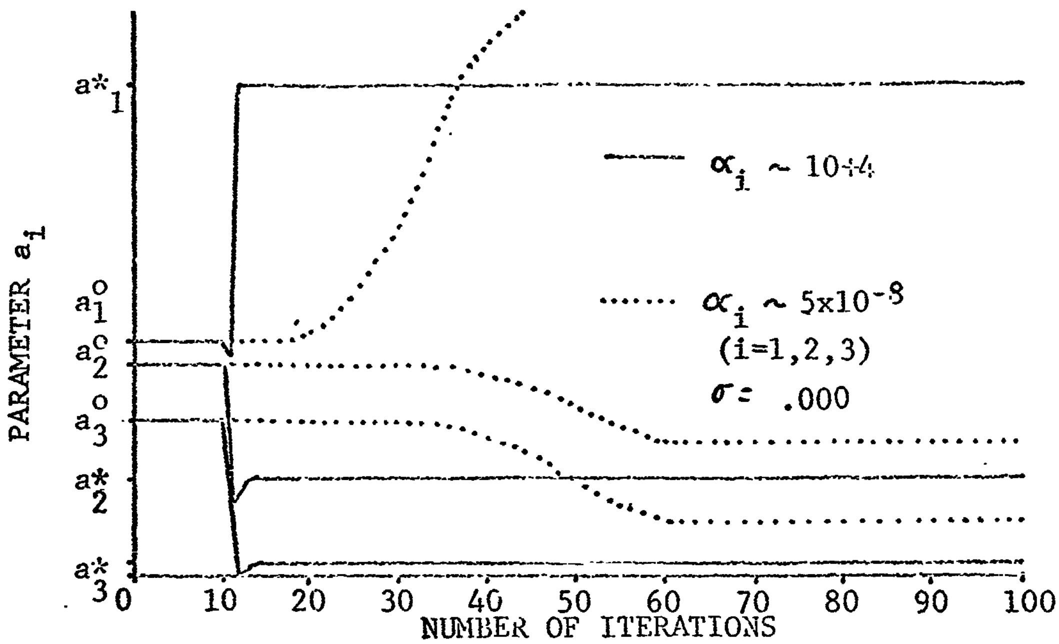

Figure 1

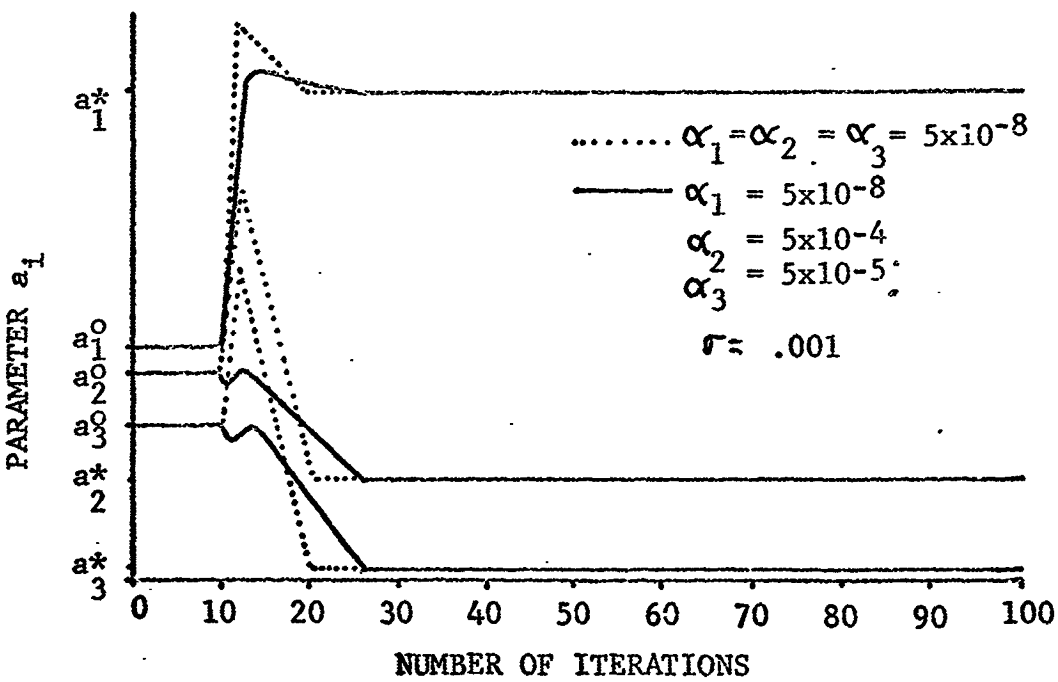

Figure 2

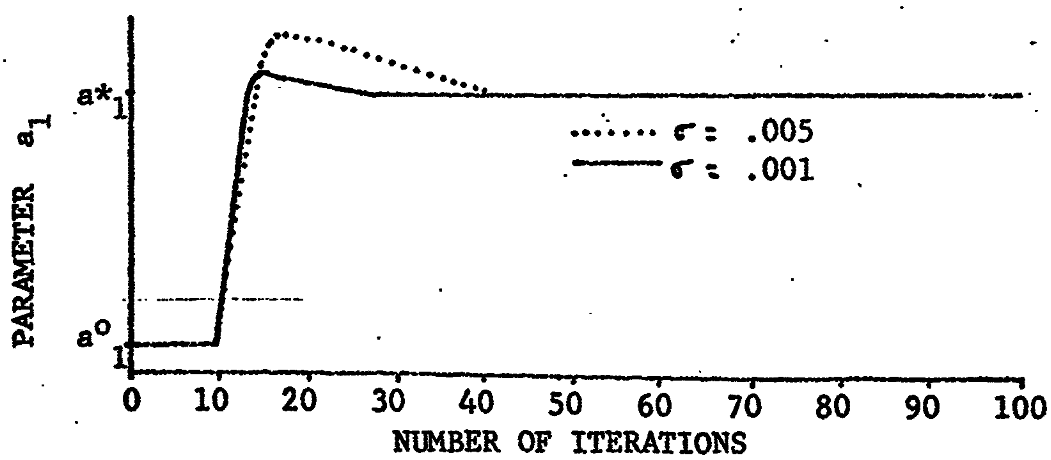

Figure 3

Figure 3 shows the effect of measurement error on the updating system. The larger standard deviation causes the overshoot to increase. It is felt that proper choice of weights will eliminate this problem.

Present research is being devoted to developing a scheme to update the weights, i.e., the α's, thus giving an on board optimal fit that will adapt to the measurements. It is expected that these studies will be joined with those of Task A.1.b. and that the combined parameter updating system will be incorporated in the adaptive trajectory control scheme, Task A.2, by the end of the next reporting period.

Task A.1.b. <u>Extension of Parameter Updating System to the Regions Above the Tropopause</u> - R.J. Carron
Faculty Advisor: Prof. C.N. Shen

Prior and concurrent work, Ref. 2, has been aimed at the development of a method to update the parameters of a modified form of the adiabatic density equation for the region defined between the tropopause and the surface for the martian atmosphere. To be of use in the design of a capsule landing system, where the capsule is to be aerodynamically braked as it enters the atmosphere, the density must also be known for the regions above the tropopause. In this region an exponential model is known to be a good estimate for the density. Therefore it is necessary to extend the atmosphere determination scheme to the regions above the tropopause.

Although it is known that the major effects of the braking force will be felt in the regions below the tropopause, where the density is greatest, an arbitrary height of 120,000 ft. above the surface of Mars has been chosen as a starting point for calculation for the density. It is anticipated that by starting the determination of the density at this height a reliable prediction of the actual density can be obtained more rapidly.

To extend the updating scheme to the regions above the tropopause, the design parameters of the adiabatic model must be correlated to a suitable set of parameters for the exponential model. The new set of design parameters would have to given reasonable estimates for the density at high altitudes where this model is more appropriate.

To accomplish this task the exponential model was put in a dimensionless form similar to the dimensionless form used for the adiabatic equation, namely;

Adiabatic Equation: $\ln \rho = A + B \ln\left[\frac{1}{N} + C(1-x)\right]$ (1)

Exponential Equation: $\ln \rho = A' + B' \ln\left[\frac{1}{N} + (x-1)\right]$ (2)

A program computes the value for A' and B' for the 2-parameter model, Eqn. 2 for the entire region of the atmosphere. The values for A' and B' from 120,000 feet to the tropopause should be constant since this is the region where the exponential model is used. The values for A' and B' in the region from the tropopause to the surface should vary according to the altitude. Although to be of use in the landing system the design parameters for the density should be constant or almost constant this scheme was looked at to see if it was possible to model the atmosphere with a two parameter equation for the entire region. It was found that the two parameter equation was ineffective.

During the next period, the proposal to represent the exponential regions of the atmosphere in terms of the three parameter model will be evaluated quantitatively for the range of atmospheric models. The effectiveness of the updating scheme, Task A.1.a, using this model will be determined.

Task A.1.c. <u>Review and Evaluation of Altitude and Density Measurement Devices</u> - J.R. Morgan
Faculty Advisor: Prof. C.N. Shen

The effectiveness of the scheme for updating martian atmosphere parameters is strongly dependent on the accuracy of the density and altitude measurements. A review and evaluation of measurement devices has been undertaken to provide support for the parameter updating tasks.

In relation to altitude measurement system, Ref. 7 and 8 both reach the conclusion that an electronically scanned pulse radar system would be most practical in view of power requirements, size and weight. The estimated measurement error depends on the size of the array decreasing as the number of elements is increased with accuracy being obtained at the cost of weight. On the basis of References 7 and 8, it appears feasible to plan for a 1% error in altitude measurement over the range from the near surface to 15 Km. For higher altitudes where accuracy must be traded off with complexity and weight, errors in the neighborhood of 2% appear to be readily achievable.

To date it appears that the gamma-ray backscattering techniques is the most feasible method for measuring atmospheric density. Reference 9 provides a detailed analysis of the device as applied to the Mars atmosphere problem. The expected system accuracy expressed in terms of a standard deviation is summarized below.

SYSTEM ACCURACY

	Altitude	
	25 km	5 km
Calibration Error:		
Pre-launch Calibration	± 3.0%	± 3.0%
Electronic Gain Variation	3.0	3.0
Heat Shield Ablation	2.0	-
Resolving Time	2.0	-
Electronic Coincidence	1.0	1.0
Atmospheric Composition	1.0	1.0
Source Strength Statistical Fluctuations:	6.6	3.8
Radiation Background Statistical Fluctuations:	4.7	0.6
Radiation Background Prediction Uncertainty:	6.5	0.8
TOTAL SYSTEM ERROR	±11.7%	± 6.0%

It should be noted that the anticipated density measurement errors are quite large in comparison to those employed in evaluating the parameter updating scheme, Task A.1.a, and that additional effort in both the measurement and parameter updating systems is in order.

Task A.2. Adaptive Trajectory Control

Principal efforts have been directed along two lines. The first of these has been concerned with the development of methods by which to compute the effects of both density parameter deviations and retro-propulsion control changes and has resulted in the formulation of a technique based on sensitivity analysis. The second line of effort has considered trajectory control in terms of discrete variation of the ballistic coefficient.

Task A.2.a. Sensitivity Guidance for Entry into an Uncertain Martian Atmosphere - P.J. Cefola
Faculty Advisor: Prof. C.N. Shen

The objective was to develop a guidance scheme which would result in a reference terminal condition, i.e. capsule velocity and range angle at a specified altitude, whatever the actual atmosphere encountered on Mars entry. It is assumed that an on-board system for updating atmosphere parameters is available.

Sensitivity Analysis is applied to the entry dynamics in order to compute the effects of both density parameter deviations and control changes. After the atmospheric parameters are tracked, the control is determined on-board by using the sensitivity coefficients previously compiled. Control updating is provided by introducing a new sensitivity equation which reduces the on-board computation since all the required terminal sensitivity coefficients are now produced by the solution of one equation. Numerical simulation assuming a VM-2 reference density and VM-1 actual density showed that the terminal velocity and range angle errors were reduced by at least 90% in comparison with those resulting from the uncontrolled VM-1 trajectory. The effects of delays in obtaining information describing the actual atmosphere and of inaccuracies in that information were also investigated.

Second order sensitivity functions are investigated with a view towards improving guidance system performance in the case of large deviations in the atmospheric parameters. Previous workers have derived higher order sensitivity equations using a single n-th order differential equation to model the physical system. However, the state vector described by n first order equations gives a more general approach for dynamical systems. A new vector-matrix differential equation for the second order sensitivity coefficients of a general system is obtained. It is found that the second order sensitivity forcing function depends on the present altitude in a planetary entry problem in contrast to the first order sensitivity forcing function which is independent of the present altitude. This point is important in the calculation of the terminal values of the second order sensitivity coefficients. With the first order coefficients, it was possible to describe all the terminal values by using the adjoint sensitivity equation. For the second order coefficients, this procedure is only possible for a certain approximation to the second order sensitivity forcing function.

Ref. 10 describes in detail the development and application of the proposed guidance scheme. Ref. 10, which is Cefola's doctoral dissertation, is now in process of reproduction and is scheduled to be released by March 30.

Task A.2.b. Discrete Variation of Ballistic Coefficient - L. Hedge
Faculty Advisor: Prof. C.N. Shen

The Mars entry guidance problem is complicated by the uncertainty which exists in the Martian atmosphere. The trajectories obtained by applying aerodynamic braking are particularly sensitive to deviations in the parameters and the parameter deviations may be quite large. Therefore, the guidance system must be able to compensate for atmospheric parameter deviation if the capsule is to meet predetermined terminal conditions necessary for a soft landing.

In order to decrease the fuel consumption, it may be possible to control the flight of the vehicle using a discrete change in the value of the ballistic coefficient, (m/C_DA). By deploying a greater effective area of drag at an appropriate altitude, it will be possible to alter the terminal values of the state variables (velocity, range, and flight path angle) and possibly, to meet the terminal constraints.

An estimate of the desired constraints for the entry phase of the mission were outlined by Ref. 11. For this investigation, the desired final conditions are taken to be a final velocity of less than one thousand (1000) feet per second at an altitude of twenty thousand (20,000) feet, and a minimized range deviation from a reference value yet to be determined.

It is important to know the effect of a change of the ballistic coefficient on the unpowered aerodynamic flight of the vehicle. Therefore, the initial phase of this investigation has been a trajectory study to determine the result of changing the effective area of drag on the final values of the state variables.

The equations of motion, assuming 1) two dimensional flight, 2) a spherically symmetric planet, 3) a non-rotating atmosphere, and 4) ballistic entry without lift, are given as follows with a normalized altitude as the independent variable*:

* Modified form of the equations of motion derived in Ref. (10).

$$\frac{d\cos\theta}{dx} = \frac{h}{R_o N}\frac{\cos\theta}{v^2}\left\{\frac{1}{\left[1+\frac{h}{R_o}\left(1-\frac{x}{N}\right)\right]^2} - \frac{v^2}{1+\frac{h}{R_o}\left(1-\frac{x}{N}\right)}\right\}$$

$$\frac{d\,v^2}{dx} = -\frac{1}{N}\frac{A}{A_o}\left[\frac{p_o\,h}{\left(\frac{m}{C_D A_o}\right)}\right]\left(\frac{e^a}{p_o}\right)\left[1+c(1-x)\right]^b \quad \frac{v^2}{\sin\theta}$$

$$+\frac{h}{R_o N}\frac{2}{\left[1+\frac{h}{R_o}\left(1-\frac{x}{N}\right)\right]^2}$$

$$\frac{d\Omega}{dx} = \frac{h}{R_o N}\frac{\cot\theta}{1+\frac{h}{R_o}\left(1-\frac{x}{N}\right)}$$

where $x = \left(\frac{h-y}{n}\right) N$ $\qquad v = \frac{V}{g_o R_o}$

and y = altitude
θ = flight path angle
V = magnitude of velocity
Ω = range angle
x = normalized altitude
v = normalized velocity
h = reference altitude
N = scale height
g_o = surface gravitational acceleration
R_o = radius of Mars
A = actual area of capsule
A_o = reference area of capsule
m = mass of entry capsule
C_D = coefficient of drag
p_o = reference surface density
a = natural log of actual surface density
b,c = atmospheric density parameters

In Martian entry, the region of importance in atmospheric braking has been considered to be below one hundred thousand (100,000) feet in altitude. The flight of the capsule in this region was simulated on a digital computer. Some of the calculated results of changing the value of the ballistic coefficients from a reference value by varying the effective area of drag are shown in Figures 4 through 7 assuming CO_2- rich martian atmosphere models

Figures 4 and 5 show the effect of the discrete change in the drag on the final value of the velocity as a function of the altitude at which change occured. Of primary importance is the fact that all the final velocities are less than one thousand feet per second, independent of atmospheric model. It is also important to note the flat portion of all the curves for different atmospheres and different changes in the ballistic coefficient. For a specific atmospheric model, the value of the final velocity is invariant if the ballistic coefficient is changed above a threshold altitude of approximately fifty thousand (50,000) feet.

Figures 6 and 7 show the effect of drag control at specific altitudes on the flight range angle of the capsule. The significant point from these curves is their symmetry. If the ballistic coefficient is changed at a specific altitude, the amount of range deviation from the original trajectory is independent of the actual atmosphere. The deviation is purely a function of the size of the change in area.

Now consider both the final velocity and the flight range for a specific area change. If the change of area is sufficiently large, there is an overlapping region (for the atmospheres considered) of both the final velocity and the flight range Figures 5 and 7. Assume, for example, that a VM-4 atmosphere without any change in the ballistic coefficient is chosen as a reference. Then, if a different atmosphere is encountered, it is possible to find an altitude where changing the ballistic coefficient will result in the specified terminal velocity. Similarly, it is possible to match the flight range by changing the ballistic coefficient at an appropriate altitude.

From basic control theory, the change of area as a control can only be used to effect one state variable. However, a compromise seems possible so that the specified terminal conditions can be met for both range and velocity. The velocity can be considered as an inequality constraint. For a ballistic coefficient of .3 or less, the terminal velocity is below one thousand (1000) feet per second. If the change of area takes place above fifty thousand (50,000) feet, the velocity would meet an even tighter constraint of a VM-4 reference. Therefore, it seems that the change in the ballistic coefficient can be used to make the vehicle hit a reference range point and in addition, the velocity inequality constraint will also be met.

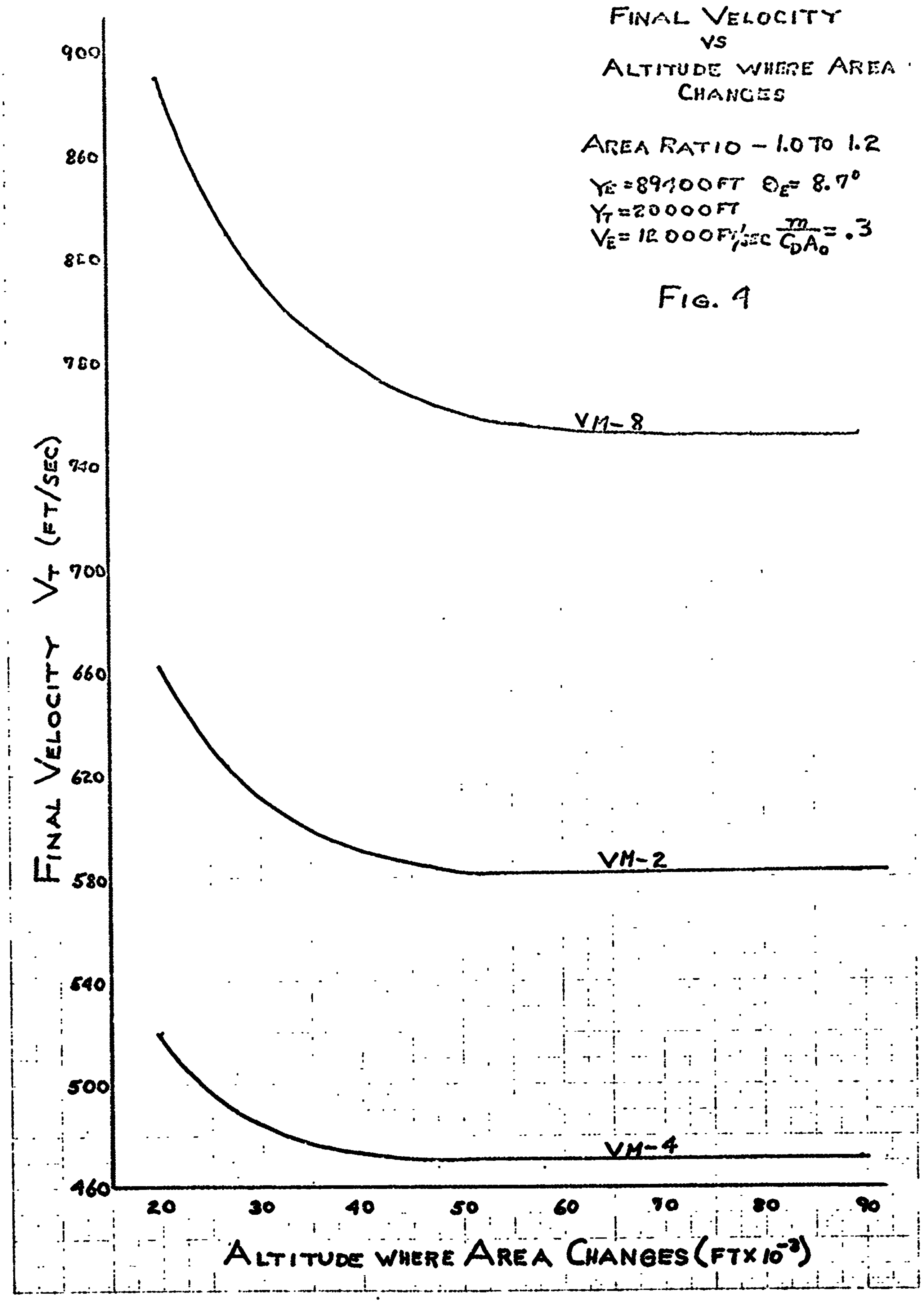
FINAL VELOCITY
VS
ALTITUDE WHERE AREA
CHANGES
AREA RATIO – 1.0 TO 1.2
Y_E = 89100 FT Θ_E = 8.7°
Y_T = 20000 FT
V_E = 12 000 FT/SEC $\frac{m}{C_D A_0}$ = .3
VM-8
VM-2
VM-4
900
860
820
780
740
700
660
620
580
540
500
460
20
30
40
50
60
70
80
90
FINAL VELOCITY V_T (FT/SEC)
ALTITUDE WHERE AREA CHANGES (FT x 10^{-3})

FIG. 4

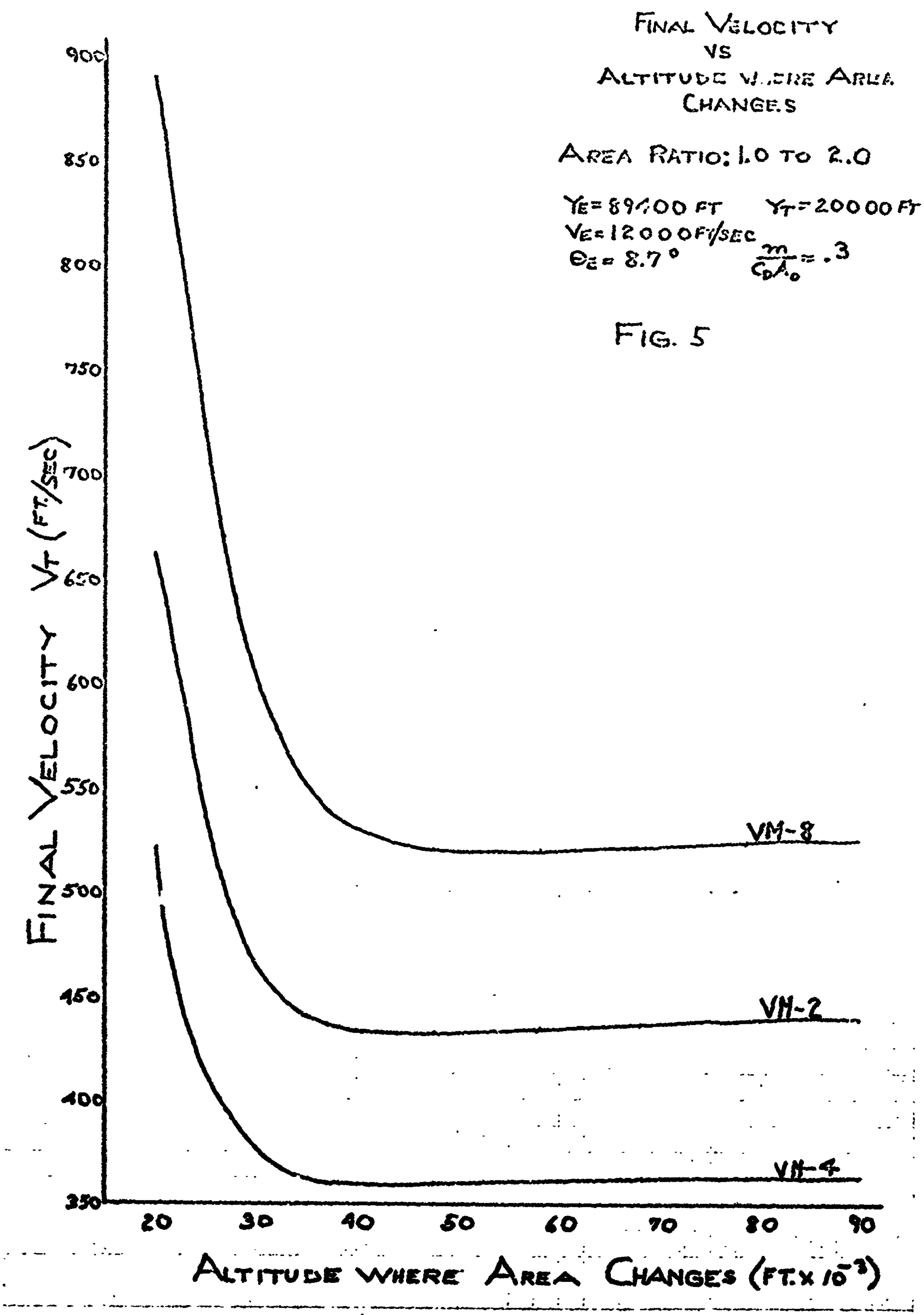
FINAL VELOCITY
VS
ALTITUDE WHERE AREA
CHANGES
AREA RATIO: 1.0 TO 2.0
YE=89400 FT   YT=20000 FT
VE=12000 FT/SEC
ΘE= 8.7°   m/CDA0 = .3
900
850
800
750
700
650
600
550
500
450
400
350
FINAL VELOCITY VT (FT/SEC)
VM-8
VM-2
VM-4
20
30
40
50
60
70
80
90
ALTITUDE WHERE AREA CHANGES (FT. x 10^-3)

FIG. 5

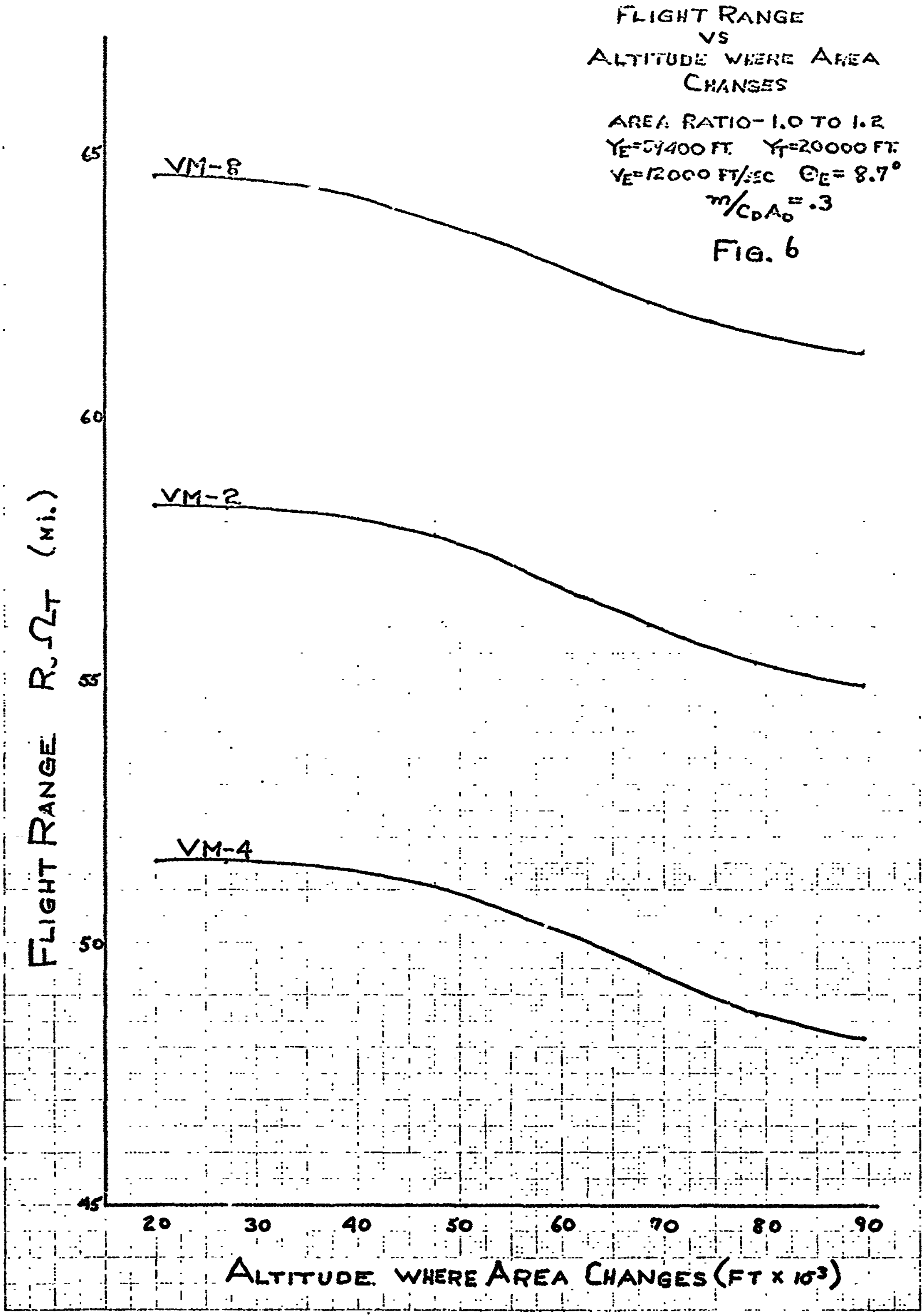
FLIGHT RANGE
VS
ALTITUDE WHERE AREA
CHANGES
AREA RATIO- 1.0 TO 1.2
Y_E=59400 FT. Y_T=20000 FT.
V_E=12000 FT/SEC Θ_E= 8.7°
$m/C_D A_0$= .3
VM-8
VM-2
VM-4
65
60
55
50
45
20
30
40
50
60
70
80
90
FLIGHT RANGE R, Ω_T (MI.)
ALTITUDE WHERE AREA CHANGES (FT x 10^3)

FIG. 6

FLIGHT RANGE
VS
ALTITUDE WHERE AREA
CHANGES

AREA RATIO: 1.0 TO 2.0

$Y_E = 89400$ FT $Y_T = 20000$ FT
$V_E = 12000$ FT/SEC
$\theta_E = 8.7°$ $\frac{m}{C_D A_0} = .3$

FIG. 7

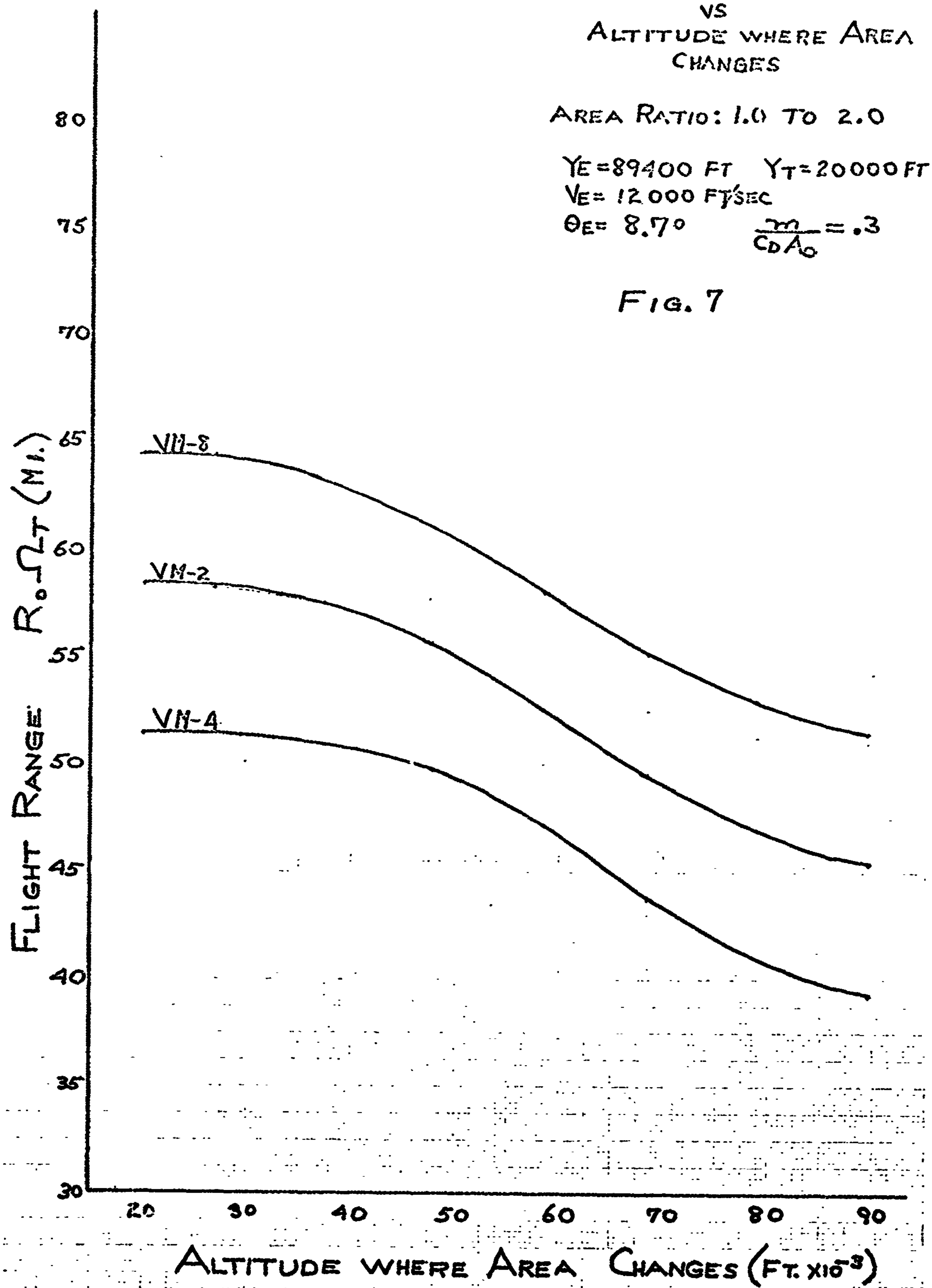

However, as a working guidance scheme, this solution to the problem has a certain limitation which must be kept in mind. The amount of area change must be determined by the lowest density atmosphere possible. The results given here assumed the VM-8 atmospheric model represents the lowest density profile that is to be anticipated. Simulation shows that doubling the effective area allows the vehicle to meet the VM-4 reference terminal conditions. However, if an atmosphere of lower density were to be encountered, the final constraints would not be met. Therefore, a lower limit on the density must be known for such a guidance scheme to succeed.

Presently, the effect of changing the ballistic coefficient at higher altitudes is being investigated. This change should just extend the flat portion of the final velocity curves. However, this change should allow for a greater overlapping of the flight range curves. The feasibility of this control scheme for the nitrogen-rich martian atmosphere models will be determined. This scheme will be compared to the alternative described under Task A.2.a.

Task B. Unpowered Aerodynamic Landing

Accomplishing a soft landing on the planet Mars can be a particularly difficult mission, Ref. 12. The atmosphere of the planet is so tenuous (surface density on the order of 100-th the density of that of Earth's) that the techniques employed for Earth re-entry seem by themselves inadequate. These proposed methods of soft landing usually employ a large, blunt body for entry, parachute, balloon, or deployable wing for descent, and retrothrust rockets for soft touchdown.

The combined weight of such a system would tend to preclude the development of small landing capsules due to a very unfavorable payload fraction. On Mars the difficulties are aggravated by the existence of extremely high surface winds (200 ft/sec. with higher gusts). A soft landing capsule must be able to counteract these winds so as to land at zero ground speed. While flight into a headwind at zero ground speed would impose extra fuel requirements on a retrothrust-supported landing vehicle, it will actually improve the performance of a device which employs aerodynamic lift for support, such as the autogyro.

The unpowered rotary wing, which seems to be the best aerodynamic means of providing the deceleration during descent and of countering the surface wind, offers the advantage that kinetic energy can be stored in the rotating hub and wing assembly. This makes it possible to hover briefly before touchdown without expending fuel, and make contact with the ground very gently.

This task involves a number of phases which are considered separately below and includes problems in: descent simulation, analysis of transient blade motion, hub design, blade pitch control system, design and fabrication of inflatable blade section, and aerothermoelastic blade analysis.

Task B.1. Descent Simulation Including Transient Blade Analysis and Pitch Control System - T.N. Kershaw
Faculty Advisor: Prof. G.N. Sandor

Ref. 3, which summarized prior work, presented the results of a descent simulation model for the case of untwisted blades for a capsule in axial flight. One major technical weakness in the simulation model was due to assumptions made regarding the rotary wing start-up thrusts. In addition, the mathematical expressions for the lift and drag coefficients were not of sufficient accuracy over the whole range of angle of attack.

Efforts have been undertaken in order to correct these shortcomings. The solution to the start-up problem is being sought through modification of the descent computer program, Ref. 3, to allow an accurate calculation of the coning angle based upon the flight conditions and the blade parameters assuming the use of a light-weight rotor. The modified scheme computes the coning angle based upon an accurate solution for the equilibrium position reached by the blade when acted upon by aerodynamic-force, weight, and spring-restraint moments. This analysis simulated by a digital computer was based on a hub assembly with no spring-restraint moment. This resulted in coning angles at start-up which were so large they could not produce any appreciable thrust. Thus as the program is being incorporated into the descent simulation, various values of the flapping hinge spring constant are being investigated. Once an appropriate value is determined for the hinge spring constant, it will be used as an input to the design of the rotor blade. Also, with respect to the design of the blade, loading curves will be found so that the necessary rigidity can be designed into the blade in order to keep deflections along the blade within acceptable limits.

15th order Fourier series representation of the lift-drag characteristics of the airfoil have been developed but time has not permitted their incorporation in the descent simulation. The simplest method for applying this representation is being sought and its evaluation is indicated for the near future.

The descent simulation which is proposed is based on a steady state blade element analysis for an autorotating lifting rotor taken in time steps. The accuracy of the steady state assumption has not as yet been proven. To this end, it has been proposed to use the numerical method of solution for the transient blade motions reported in Ref. 13. The model of the hub assembly used in Ref. 13 fits our situation and a computer scheme to implement this scheme is being developed. As soon as the difficulties in the descent simulation program are resolved, emphasis will be shifted to implementation of this analysis. Since both analyses are based upon a blade element analysis, this scheme should lead to a definite check on the results of the steady-state analysis for the untwisted blade in axial flight. The use of the transient blade motion analysis is expected to be limited to the application as a check on the accuracy of the steady state analysis and the resolution of the question of the applicability of the step-wise use of the steady state analysis.

All of these analyses of descent simulation have as their control parameter the hub pitch angle. For this reason a basic control stability analysis was undertaken early in this period of work. This control analysis assumed a rigid blade as do the aerodynamic analyses. This of course means that aerothermoelastic effects have been neglected. The results of this study could not be in as definitive a form as might be desired since the design of the blade is still in a preliminary stage, but the relationships which were obtained will be used in the development of the blade design. As one result, it was concluded that there should not be any backlash in the mechanical pitch control unit if a continuous controller is to be used. Since the proposed controller is an A-C fluidic master-slave system, care must be taken to satisfy this requirement. The problem of aerothermoelastic effects, Task B.5 is now under study and the results which are obtained will influence both the pitch control and descent simulation tasks. Also at this time the mechanical portion of the pitch control unit is being developed and it is planned to employ a fluidic system such is are represented in Figure 8. The A-C fluidics which have been developed commercially can be applied to this position control system. One such system operates using the master-slave relationship. The master resonator will be located inside the hub assembly. It consists of an oscillator in connection with a phase discriminator and a slave piston which follows the

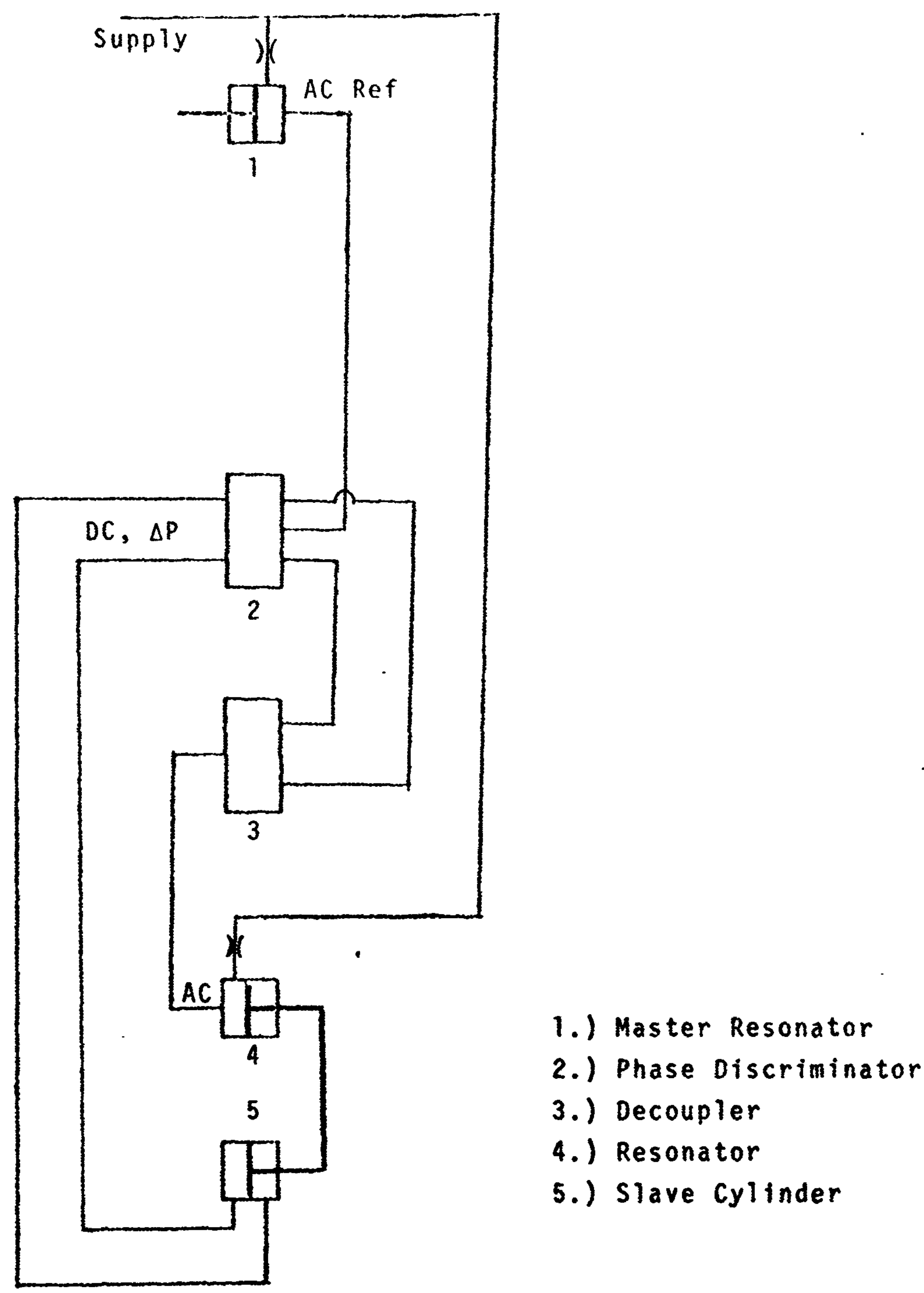

Figure 8. Schematic: Fluidic Pitch Control Unit

motion of the master piston. The circuit is such that the slave moves to keep the slave frequency equal to the control frequency. The basic element of the system, the phase discriminator circuit, is commercially available.

During the next reporting period it is intended to:

1. Complete the descent simulations based on the rigid blade assumption and including a 15-th order Fourier-series representation of the lift and drag coefficient data. Axial and forward flight conditions will be simulated.

2. Combine the transient blade analysis with descent simulation with emphasis to the start-up problem.

Task B.2. <u>Autogyro Rotor-Hub Assembly Design</u> -
W. Parker Rayfield
Faculty Advisor: Prof. G.N. Sandor

The objective of this task is the design of the rotor hub assembly for the autogyro landing system. In addition to meeting the strict strength, weight, and environmental requirements, the hub must also be capable of performing all the necessary control and monitoring functions.

The initial weight allotment of five pounds for the entire hub assembly requires a much simpler design than that of the standard autogyro or helicopter. The axial load at 12 G's is 500 pounds and the maximum radial load per blade is 650 pounds; this high strength-to-weight ratio greatly complicates the structural design. The vacuum of space precludes the use of normal lubricants and requires specially designed bearings and hinges. The design must also withstand the wide temperature range and radiation in space, and the martian atmosphere and pre-launch sterilization. Another requirement, common to all types of rotor hubs, is the transmission of control and monitoring signals through the revolute bearing link between the rotating hub section and the fixed capsule body.

The major component of the hub assembly is the rotor bearing. Because of the load and speed requirements and the lubrication restrictions, a hydrostatic gas bearing was chosen. This would operate by supplying a gas, such as helium or carbon dioxide, under pressure to a narrow gap separating two thin, high-strength alloy, conical shells.

The outer shell, attached to the blades, would rotate about the fixed inner shell, the pressurized gas lubricating and carrying the load between the cones.

An early concept with a single gas outlet soon gave way to a double outlet as dictated by the hub geometry. However, an enlarged cone design reduced the required gas pressure from 100 psi to 6 psi; the storage volume decreased from 18 cubic feet at 20 psi to 7 cubic feet at 6 psi. These calculations proved the gas-bearing concept feasible. A porous resistor was added between the gas supply and bearing gap to allow for varying loads. As the load decreases, the pressure drop across the resistor increases, lowering the pressure in the bearing gap. Likewise, as the load increases, the pressure drop across the resistor decreases, increasing the gap pressure. This greatly reduces the gas flow rate and storage volume necessary.

Should the blade forces momentarily reverse, tending to separate the two cones, the loading would be carried by three reversal bearings. These teflon-encased ball bearings would be attached to the top perimeter of the inner cone and support the outer cone via a nylon roller surface along its upper edge. These self-lubricating bearings would suffice for the predictably short-duration load reversals.

Solid lubricant bearings are also being used as back-up bearings, should the hydrostatic gas bearing fail. Actuated by sensitive rolamite force generators, these bearings would pivot onto a nylon roller surface, using the same support structure as the reversal bearings; they would thus separate the conical shells and support the rotor, preventing the possible binding of the gas bearing surfaces.

The blade functions require three degrees of freedom. They must be able to flap freely in the plane through the rotor axis (coning angle), rotate through a limited small angle about a vertical axis (lead-lag angle), and rotate about their own axis (pitch angle). Again the limitations of lubricating in space restrict the design. Lightweight polypropylene and polystyrene integral hinges were chosen here. The former offers free motion with no friction surfaces; the latter includes the spring constant necessary in the lead-lag hinge. The flapping hinge is inboard of the lead-lag hinge to allow monitoring of the coning angle. The collective pitch angle control mechanism is located outboard of the lead-lag hinge. An alternative to the double hinged configuration discussed above is a flexible shaft concept now receiving detailed study, Task B.3.

The cyclic pitch control in classical rotor design involves a swashplate and cam mechanism; because of friction and weight this was impractical. An alternative method, which was chosen, is to tilt the entire rotor hub about its own axis; this automatically provides the cyclic pitch changes required. Since the tilt bearings and control mechanism can be located within the pressurized capsule, there are fewer restrictions on their design.

A major requirement of the rotor hub is the monitoring of the coning angle. Since the revolute bearing would require impractical slip-rings to relay electrical impulses to the capsule computer, a mechanical indicator has been investigated, as follows. A central indicator, collinear with the rotor axis, slides along its vertical axis to indicate the coning angle. Initially the top of the rod was attached to the blade pitch-control segments by three plastic-hinged spars and rotated with the blades; the lower section of the rod contained a revolute joint attached to a fluidic cylinder position-monitor within the capsule. However, this design would not allow for cyclic flapping of the blades. The upper section was thus redesigned, replacing the plastic hinges with ball-slot slides, and joining the spars to the rod head with springs. This allows the cyclic flapping and also averages the coning angles of the three blades.

The collective pitch fluidic control system, described under Task B.1 requires that two signals be transmitted from the capsule to the rotating mechanism: a supply pressure and a reference pressure. As presently envisioned the lubricating gas will be bled through the outer gas-bearing cone at the central chamber yielding a varying, but above minimum, fluidic supply pressure to the rotating control devices. The coning angle indicator rod will actually be of tubular construction replacing the revolute joint with a swivel seal. This will allow the reference pressure to be transmitted from the fixed capsule input to the rotating control system. The fluidic control elements that comprise this system will be mounted on the outer cone structure. An alternative design would provide that a small compressed gas supply be attached to the spinning rotor as the supply pressure, eliminating one revolute link.

The initial weight analysis of the entire rotor hub assembly was approximately 20 pounds. By reducing the angle of the main bearing cones, the heaviest components of the design, and retaining the same projected area and thus the same vertical load capacity, the weight was reduced by four pounds, at the cost of an enlarged gas supply. Redesign of the pressurized inner cone further reduced the weight by three pounds. The present weight estimate is at thirteen pounds, eight pounds over the initial pre-design estimated allotment. This estimate will be periodically updated as the design progresses. Some of the details of the design are shown in Fig. 9 with the legend identifying components listed in Table 1.

Task B.3. Blade Support and Pitch Control System - R. Wepner
Faculty Advisor: Prof. G.N. Sandor

The objectives of this task include the design of the blade support configurations. Two alternatives are under consideration, namely an arrangement with separate lead-lag and flapping hinges, and a flexible shaft concept. In the hinge configuration, which was the original concept and which is shown in Fig. 10, the hub is connected to the flapping hinge, relieving moments about the vertical axis, while the addition of the flapping hinge eliminates moments in the horizontal axis. The pitch control system is located beyond the second hinge and is connected to the blade by an appropriate shaft.

The design of the shaft involves consideration of several parameters: determining the density and the modulus of elasticity for the material of construction, the length, and finally the cross section: solid or hollow shaft. There are two major factors which had to be considered. One was the deflection of the shaft at the loaded end. With this factor above in mind, the shaft would be fabricated of a very strong metal, such as molybdenum, with a modulus of elasticity of 48 x 10^6 psi; it would be made as short as possible because deflection varies with the cube of the length, and would be very thick in cross-section to increase the moment of inertia and produce small deflections.

The other factor to be considered was weight, which must be minimized. Accordingly, a very light material, such as aluminum, with a density of .098 lbf/in^3, and a short shaft with a small cross-section would be indicated.

It is seen that while both basic factors call for a short shaft, they are in opposition otherwise and a process of optimization is in order.

The alternative concept of the flexible shaft, Fig. 11,

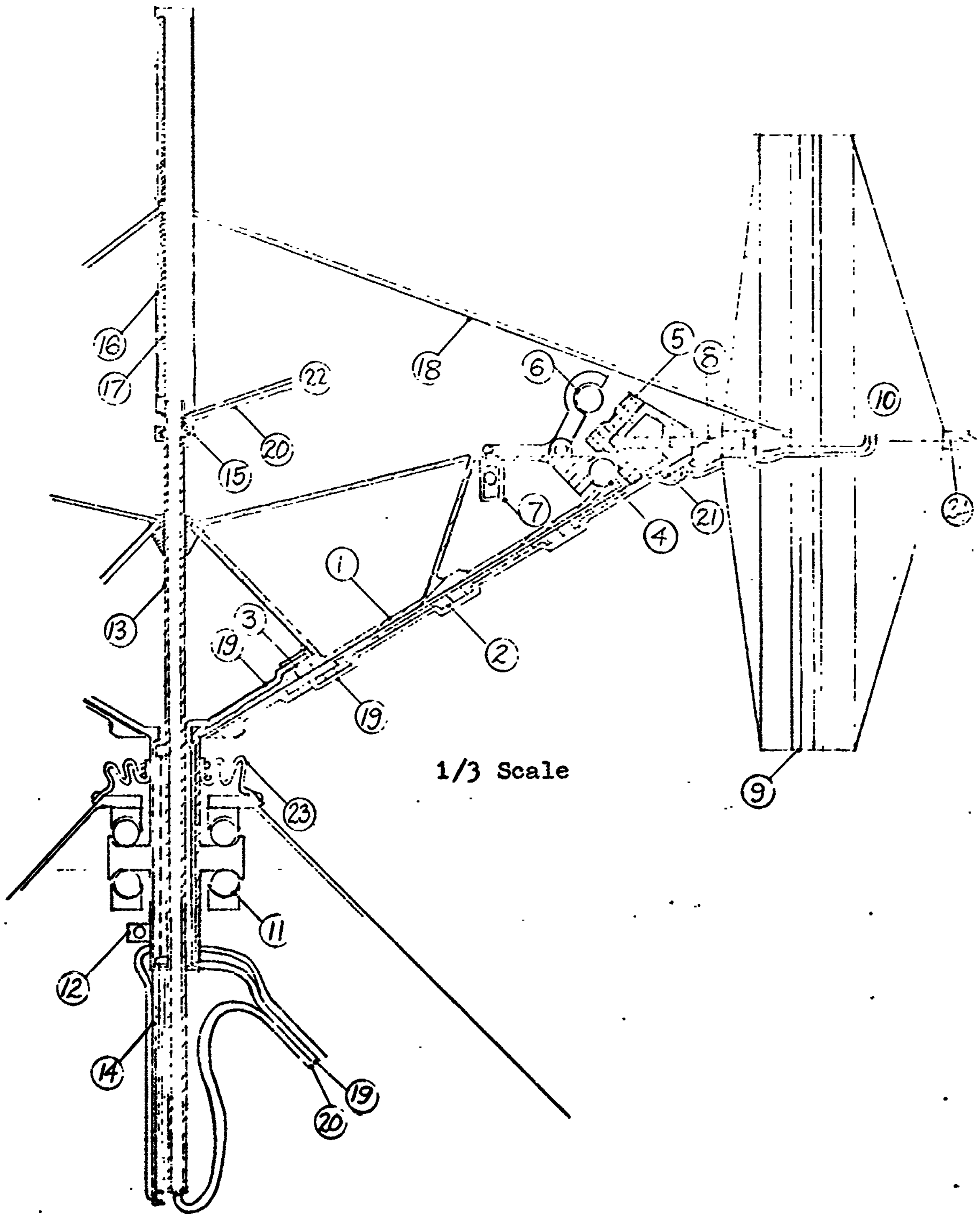

Fig. 9. Details of Proposed
Rotor Hub Assembly

Table 1. Legend for Figure

1. Hydrostatic gas bearing - inner cone structure
2. Outer cone structure
3. Porous gas resistor
4. Reversal bearing
5. Nylon roller surface
6. Back-up bearing
7. Rolamite force generator
8. Polypropylene flapping hinge (axial view)
9. Polystyrene lead-lag hinge (side view)
10. Mounting area for collective pitch control mechanism
11. Cyclic pitch control, hub-tilt bearing
12. Hub tilt-actuator mount
13. Coning angle indicator rod
14. Indicator tube
15. Swivel seal
16. Ball slot slides - indicator head
17. Averaging spring
18. Indicator spar
19. Collective pitch control - supply pressure tubing
20. Reference pressure tubing
21. Fluidic control element
22. (Tubing out of plane of indicator spar)
23. Capsule flexible pressure seal
24. Blade pitch axis

1. Blade pitch axis
2. Lead-lag hinge
3. Flapping hinge
4. Rotor axis
5. Hub-tilt axis
5.. 7. Coning angle indicator-
   linkage hinges
8. Blade pitch adjusting
   servo.

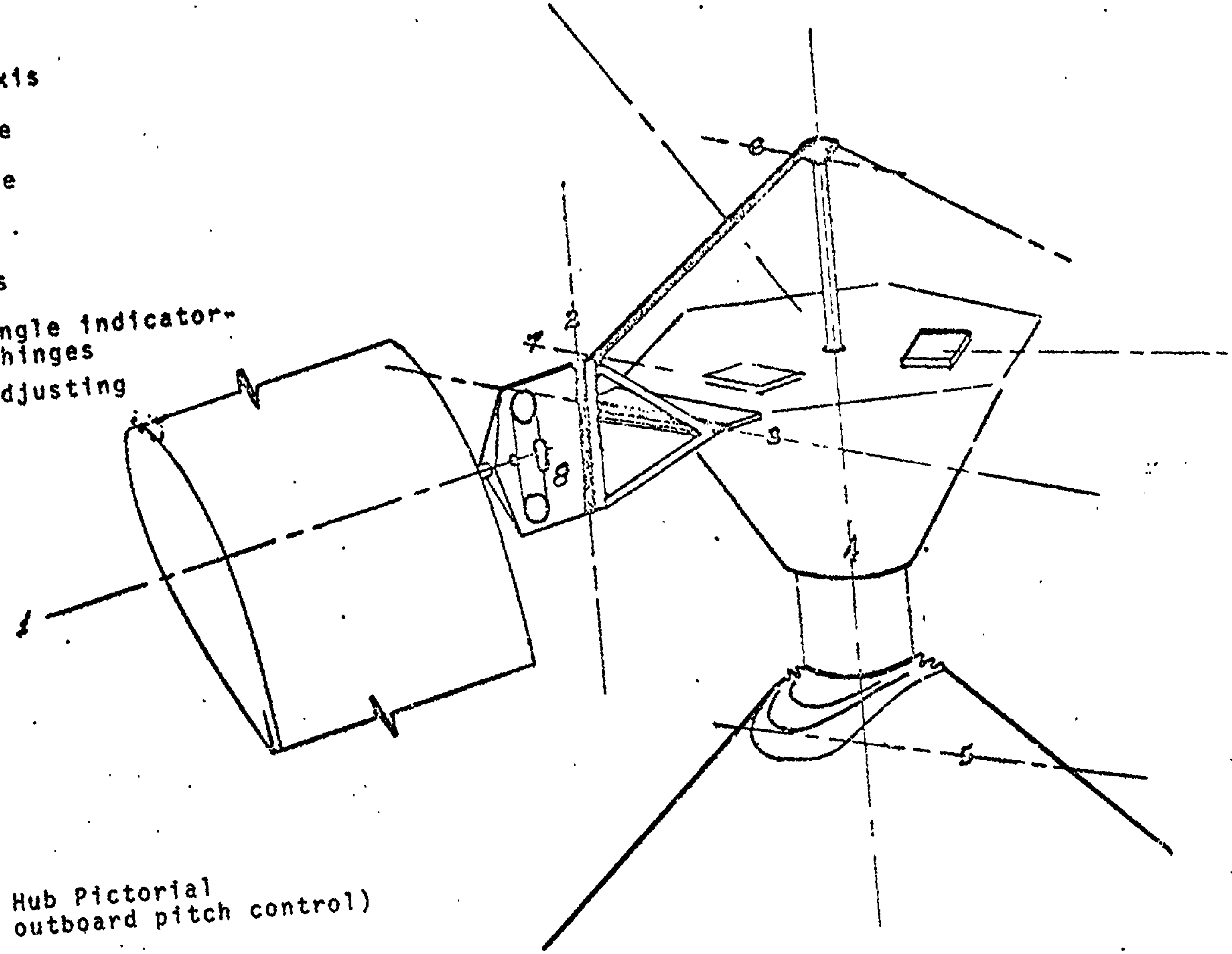

Fig. 10 Rotor Hub Pictorial
(with outboard pitch control)

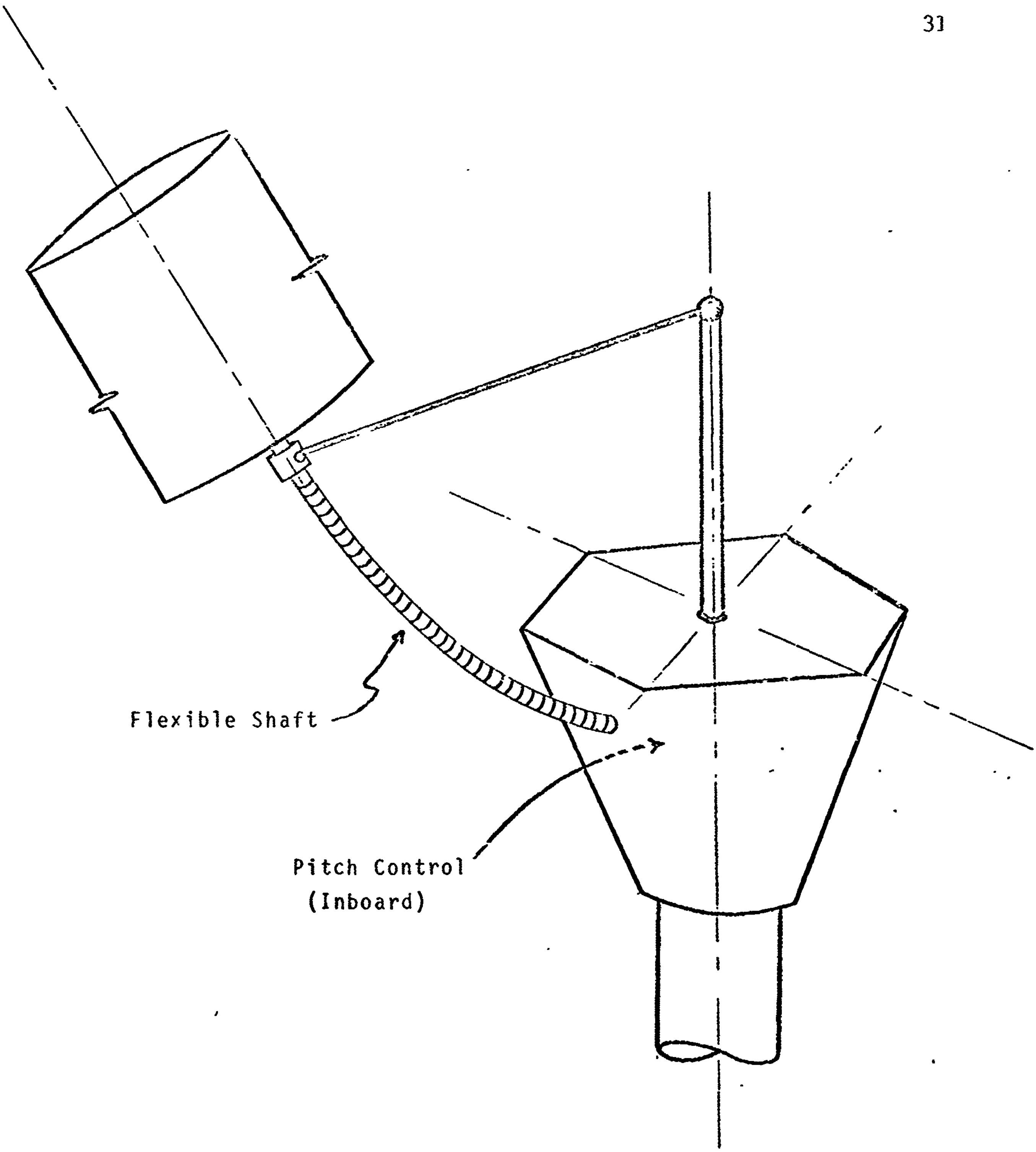

Fig. 11 Flexible Shaft Configuration

has the pronounced advantage of allowing to locate the pitch controls inside of the hub as well as simplifying the blade support configuration. The number of components is reduced, suggesting a weight advantage and increased reliability and coordination of the three blades. In addition, hollow flexible shafts would provide a direct method for inflating the blades and they would lend themselves to allowing the blades to be wrapped around the vehicle prior to deployment. Several problems must be considered before the flexible shaft concept could be chosen over the original hinge configuration. These are:

1. Unforeseen instabilities under which the shaft might buckle.

2. Modification of current coning angle indicator concept, Task B.1.b.

3. The effect of moment transmission through the shaft on the performance of the rotor. It should be noted that the hinge configuration eliminated transfer of moments, while the flexible shaft will transmit some moments.

4. The original concept permitted free travel over a limited range and none outside this range. The flexible shaft concept cannot provide this characteristic.

Effort during the next reporting period will be concentrated first on evaluating the alternative blade support configurations. Once a configuration is decided upon, emphasis will be directed to the design of the blade pitch control system.

Task B.4. <u>Inflatable Blade Model and Experimental Testing</u> - J.P. Saddler
Faculty Advisor: Prof. G.N. Sandor

Plastic inflatable blades are presently being considered for use in the Mars landing b·· autogyro. This blade concept is suggested by the space and weight restrictions on the landing capsule. These blades would be deflated and folded or wrapped around the vehicle for the interplanetary flight, and would be inflated and deployed while in the Mars entry trajectory. The present design envisions three blades, each twenty feet in length with a chord length of two feet.

A program for fabricating a blade model and testing its stiffness characteristics has been undertaken. Stiffness factors required for final design include the torque and bending moment for a unit deflection of the blade in torsion and bending, respectively. Therefore, the blade model will be subjected to torsion and to bending in both the horizontal and vertical plane, and the resulting deflections are to be measured. Since the blade stiffness will depend on the inflation pressure, the relationship between these two variables will be studied.

The period of September through December, 1968 has been devoted to an investigation of the design and fabrication of test specimens for such experiments.

On the basis of preliminary descent simulations, Ref. 3, the NCAA 0012 blade section has been chosen for fabrication and test purposes. In order to avoid end effects, a blade length of four feet has been selected for the experiment. The blade will consist of an outer shell and fourteen pressure-tight cylindrical spars varying in diameter approximately from 3/8 in. to 2-7/8 in. In order to insure the proper blade profile on inflation, adjacent cylinders must be sealed along the line of centers, and then the cylinders must be sealed to the outer shell. A typical blade cross-section is shown in Figure 12.

The blade material will be Kapton Type "F" Polyimide film with a 2 or 3 mil film thickness depending on the relative stiffness and the weight. Although the stiffness of a cylinder will be influenced more by inflation pressure than by film thickness, the latter limits the pressures which can be used. The largest cylinder in the blade model can accommodate pressures up to 20 psi and 36 psi for 2 mil and 3 mil film, respectively. Two 11.0 inch long cylinders of about 2" diameter are being fabricated, one with a 2 mil thickness and the other with a 3 mil thickness of film. If tests on these cylinders demonstrate that pressures below 20 psi will provide adequate stiffness, then the 2 mil film will be employed. Otherwise, the heavier film will have to be used.

Carbon dioxide and helium have been considered for pressurizing the blade. Since carbon dioxide is believed to be present in the Mars atmosphere, any leakage of this gas would not contaminate the atmospheric tests during the mission. Helium has the advantage of being much lighter than carbon dioxide, but the permeability of "Kapton" film for helium is approximately nine times greater than that

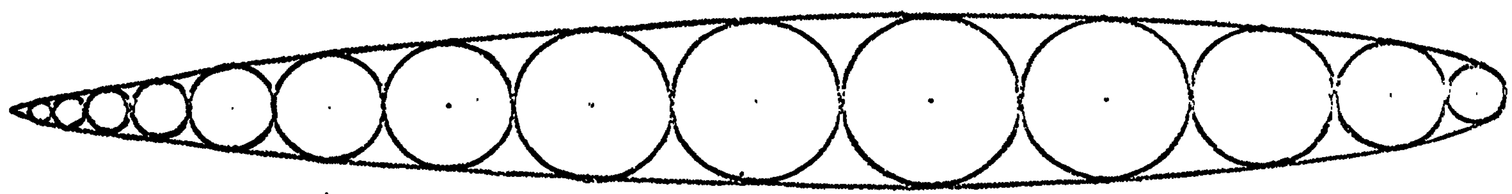

1/3 Scale

Fig. 12. Blade Section NACA 0012

for carbon dioxide (2500 cc/hr. as compared to 275 cc/hr. over the area of three blades). However, this leakage is small compared with the total volume of 600,000 cc. which suggests that the lighter gas may be acceptable.

Table 2 summarizes factors contributing to the weight of one blade using two different film thicknesses and two different pressurizing gases. The weights of all combinations are greater than the preliminary weight allotment of three pounds.

Various heat sealing applications are required in the construction of a model. First, cylinders must be formed with a pressure tight seem seal extending the length of the cylinder. Then, adjacent cylinders must be sealed together, and finally, the outer shell must be formed over the cylinders and sealed. There are several techniques for accomplishing these seals. Regardless of the technique used, the following information is pertinent to the heat sealing process, using Kapton type "F" film:

1. The optimum heat sealing temperature is 600-650°F.

2. The time of the seal is 0.5 seconds.

3. The bond is not significantly affected by variation in contact pressure.

A fabrication scheme has been conceived to satisfy the above requirements and the practical considerations.

The present plan for the coning period is to construct the first model and perhaps begin tests. This will depend, however, on the success of the heat sealing and other fabrication processes, and if any major changes are required in these areas, there will be a corresponding time delay. In preparation for the tests, investigation of means for applying torques and moments and measuring deflections will begin during this period.

Task B.5. <u>Aerothermoelastic Analysis</u> - J.V. Lazzara
Faculty Advisor: Prof. E.J. Brunelle

The objective of this task is to investigate the aeroelastic and thermal characteristics of the lightweight flexible rotary wing system which is proposed as a means of implementing an unpowered aerodynamic landing on Mars.

	(1) Weight of Kapton, lbs	(2) Weight of Helium, lbs	(3) Weight of CO_2, lbs	(1) + (2) Weight Kapton+Helium, lbs	(1) + (3) Weight Kapton+CO_2, lbs
2.0 Mil Thickness of film #200F919	3.78	0.08	0.90	3.86	4.68
3.0 Mil Thickness of film #300F929	5.24	0.08	0.90	5.32	6.14

Table 2. Contributions to Weight of One Inflatable Blade 20 Feet in Length and 2 Feet in Chord.

Work was initiated in this area in mid-November and the effort to date has been focused primarily on familiarization with the theory and methods of analysis required for the evaluation.

The aeroelastic phenomena which may cause instabilities of the proposed wing system are flutter, buffeting, dynamic response, load distribution, divergence and control effectiveness. Load distribution and divergence, which apply to the static analysis of the problem, will be investigated first.

The static analysis makes the following simplifying assumptions:

1. Perfectly elastic blade in the region under study.
2. The elastic behavior of the structure is defined in the range below the point of elastic buckling.
3. No chordwise bending.
4. Linear system.
5. The concept of an elastic axis has been introduced.

These assumptions permit a complete static analysis including the effects of centrifugal forces and aerothermal heating.

It is intended that the static analysis can be completed by April 30, 1968 and that the results can be incorporated into the descent simulation as limiting conditions. Assuming that these studies continue to support the feasibility of the rotary wing concept, efforts will then be directed into the dynamic analysis of the system.

Task C. Surface Navigation and Path Control

Following a successful landing of the roving vehicle on Mars, the problem of directing the motion of the rover from the landing size to any other specified points on the martian surface must be dealt with. Shown in Fig. 13 is a proposed configuration for a vehicle guidance system which is based on a two-level of control concept, namely, a long-range path selection with local path perturbations due to the presence of obstacles. The task of long range path selection includes terrain data acquisition

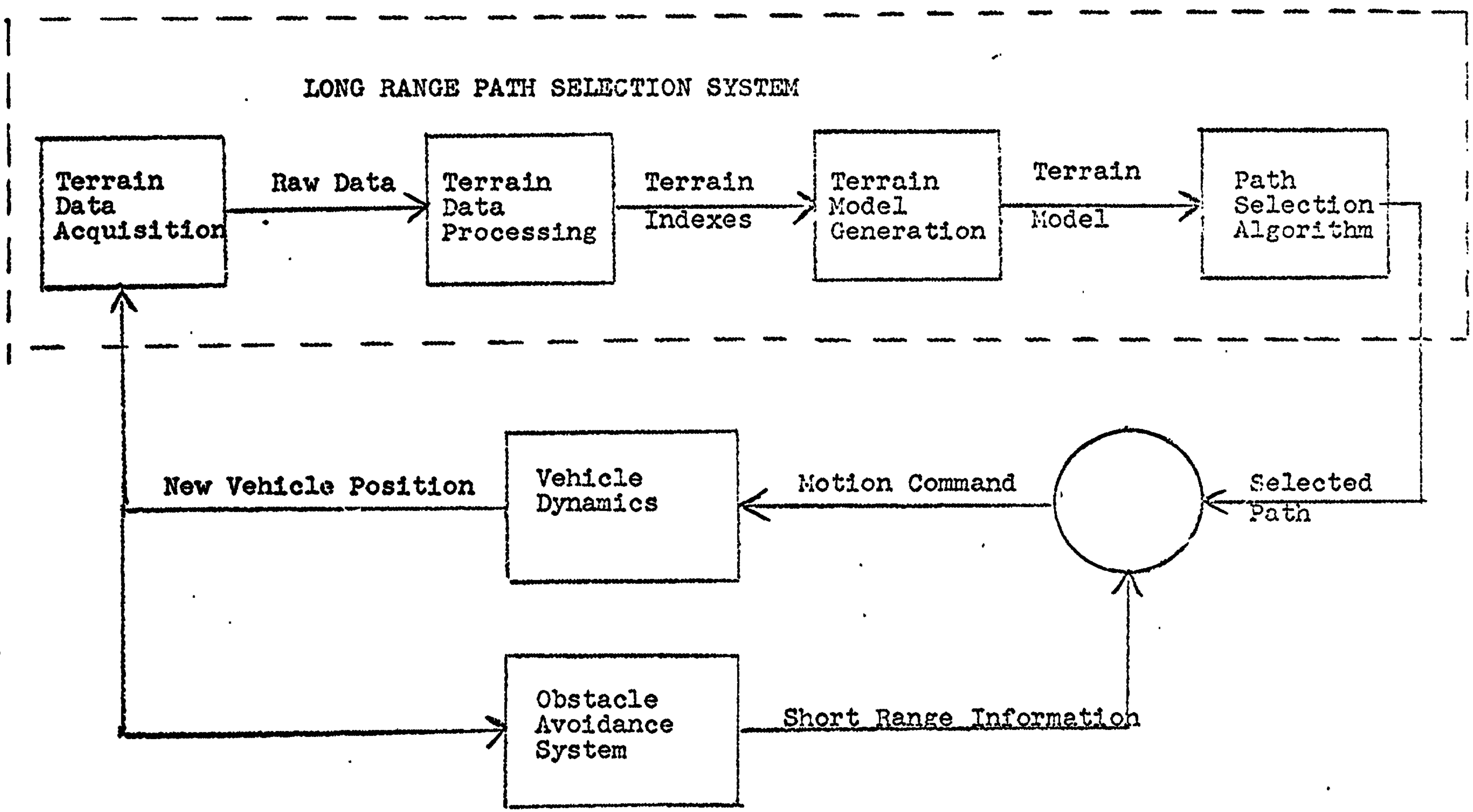

Figure 13. Vehicle Guidance System

and processing, terrain modeling and path selection and work in this area is described under Task C.1 below. Obstacle detection is concerned with the development of systems for short range detection, Task C.2, and with attitude detection since adverse slopes are "obstacles", Task D.2. Vehicle dynamics which includes questions regarding the vehicle configuration and its suspension system is taken up under Task D.1.

Task C.1. <u>Long Range Path Selection</u> - R.J. Mancini
Faculty Advisor: Prof. D.K. Frederick

The roving Martian vehicle must use some "built-in" capability (or guidance system) to independently direct its motion toward a predetermined destination. The guidance system has to make a decision on a specific course to take, for the most part, from information the vehicle sensor can obtain. The guidance system may use both information on a general path to travel (long range path selection) and specific information on local obstacles (short range obstacle avoidance) to make a decision. The work presented here is on the development of a long range path selection system, and has been divided into two parts: (1) development of a long range path selection system assuming an "ideal" sensor (ideal in respect to the accuracy of the sensor measurements); (2) evaluation of the path selection system considering errors in the sensor's measurements inherent in an actual sensor, i.e., radar, laser. The initial work on the path selection system has assumed use of an ideal sensor.

The long range path selection system has been delineated into four distinct but related functions. These functions have been listed below each with a bried description.

1. Terrain Data Acquisition - Information (raw data) about the terrain is obtained by the vehicle's sensor. The form of this raw data is as follows: the range (R) from the vehicle to a terrain feature at a specific azimuth angle (θ) and elevation angle (β).

2. Terrain Data Processing - The raw data is converted into indexes that mathematically characterizes the terrain surrounding the vehicle.

3. Terrain Model Generation - The indexes are used to define a terrain model. The terrain model is to be used to classify the various directions around the vehicle as hazardous, questionable, or safe for vehicle travel.

4. Path Selection - A path selection algorithm uses the terrain model and the predetermined destination to determine the best path of travel information can then be used by the vehicle's guidance system.

Emphasis has been directed to the problems of terrain data acquisition and terrain data processing. In the analysis of terrain data acquisition, it was necessary to know the type of terrain information the vehicle's sensor could acquire from actual terrain in order to insure realism. A Geological Survey Map, Ref. 14, was used as a source of data for the terrain whose average grade (slope) of most of the general terrain features was, of the order of 10 ± 5^{o}. This compares favorably with estimates of terrain slopes on Mars provided in Ref. 15.

Three types of terrain information were considered to be available, the azimuth angle (θ), elevation angle (β), and range (R) of terrain relative to the vehicle. A vehicle position was assumed on the map, then the terrain data was compiled. From this compiled data, two types of plots were made: R vs. β with θ constant, and R vs. θ with β constant.

The following results are submitted from the analysis of the terrain data:

1. The elevation angle (β) which is defined as Z/R gave an indirect measure of the altitude (Z) of terrain feature relative to the vehicle's altitude at a specific range (R). Figures 14 and 15 are examples of typical data obtained for a specific azimuth on the real terrain. Note that variations in β do not provide a direct indication of the slope of the terrain. It was also found that small increments of β were needed to get useful information (5 milliradians as a typical increment).

2. It was more difficult to obtain useful terrain information as the range (R) increased. This was due to the resolution problem of finding small changes in Z as R became very large. A maximum range of 8,000 feet was used.

3. Increments in azimuth angle (θ) were found to be not as critical as in β.

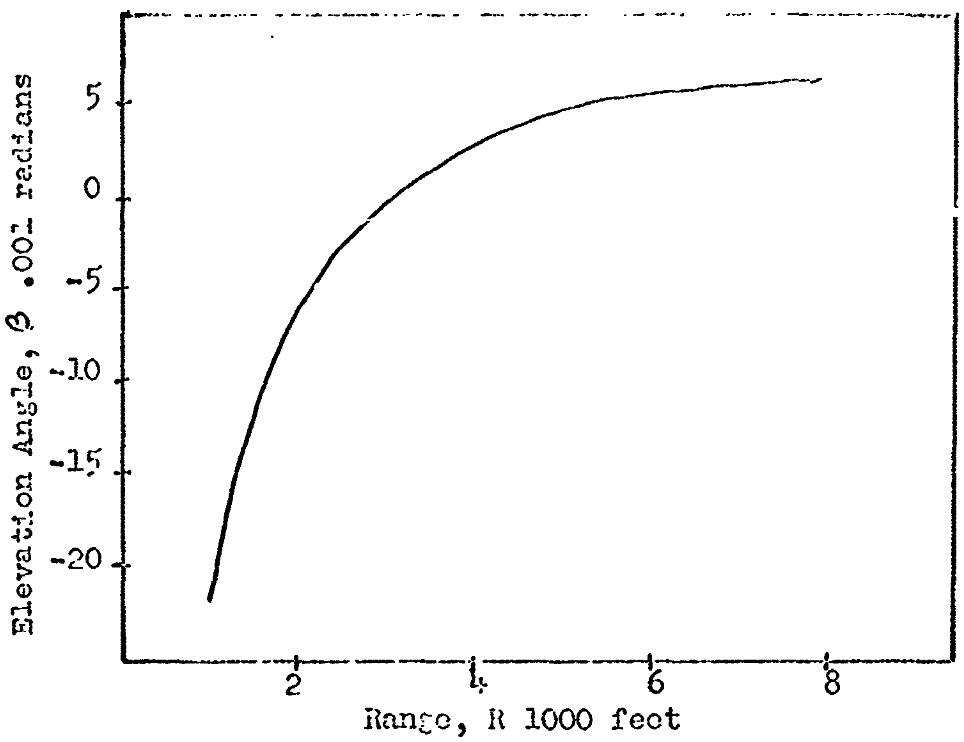

Figure 14- Range versus Elevation Angle for a fixed Azimuth Angle. These are the vehicle sensor measurements corresponding to the terrain profile in Figure 15.

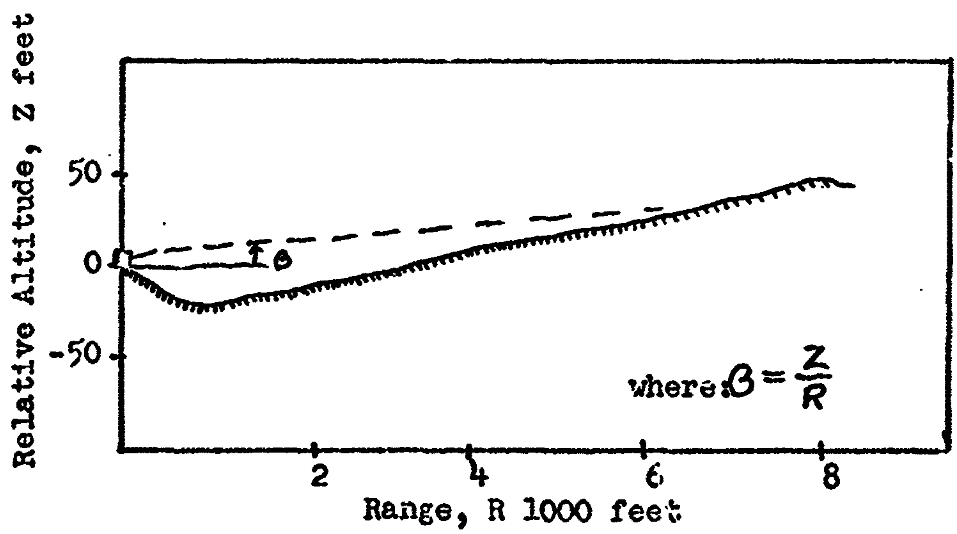

Figure 15- Sample Terrain Profile corresponding to the vehicle sensor measurements in Figure 14.

4. The best increment of ρ and Θ as well as the maximum range could not be determined from the data analysis but will depend on the work done on terrain data processing and terrain model generation.

5. Although the analysis did point out the type of information available to the vehicle through its sensor, the best paths of travel could not be determined without processing this information.

In order to process the raw terrain data, indexes were defined to permit a quantitative characterization of the terrain. The indexes being considered currently are as follows:

1. Random Variable Index

2. Discontinuity Index

3. Gradient Index

The motivation for the random variable index was to generalize the type of terrain, valley, plain, gentle slope or hill that is to be encountered in the various directions around the vehicle. The other indexes could refine this estimate. The approach used in the formulating of this index involves the observation of the variation of range with elevation angle along an azimuth. The range, R, will be treated as a random variable. Relationships between the expectation and variance of R will be obtained in order to classify the terrain.

The discontinuity index is concerned with sensing "hidden" regions (hidden in respect to the sensor's line of sight). These hidden regions represent unknown potential danger and can be treated as a type of hazard to travel. This index is computed according to the discontinuities in range as observed by the sensor in making a sweep in elevation angle along a fixed azimuth. Hidden regions are directly related to the magnitude of ΔR.

The rationale of the gradient index follows from the following arguments: If the slope of some terrain feature can be measured along as azimuth, the slope, in general, is less than the gradient of the terrain feature. The purpose of this index is to find an approximation of the gradient of the terrain feature from available sensor information. The sensor information need are as follows: (1) slope of a terrain feature along an azimuth, and (2) two measurements of range (R) and azimuth (θ) taken at the same elevation angle (β). Let the altitude (Z) be described as a function of position ($Z=f(x,y)$) as a topographical map. The "level lines" are the curves for which Z is a constant. Perpendicular to these curves are the direction of steepest descent (or gradient of Z). Once the direction of steepest descent is known, the magnitude of the gradient can be found. For use in this problem Z is taken as the altitude of a terrain feature relative to the vehicle's altitude. Partial work has been done toward the derivation of this index.

The future work will concentrate on the following items:

1. Complete the formulation of the indexes for terrain processing.

2. Integrate these indexes into a terrain-data processing system related to a terrain model.

3. Test the processing system and terrain model using a computer simulation of a terrain or a terrain modeling table.

4. Use this terrain model on existing path selection algorithms.

5. Determine the accuracy of sensor measurements and the sensor beamwidth required for the success of the path selection system.

Task C.2. <u>Short Range Obstacle Detection System</u> -
G. LaBarbera
Faculty Advisor: Prof. D.K. Frederick

The goal of a short range obstacle detection system is to alert the vehicle to the presence of obstacles which it cannot negotiate directly and to initiate maneuvers that will avoid such obstacles. Broadly speaking, obstacles fall into the categories of positive or negative obstacles, i.e., protuberances or cavities, which include the special case of adverse slopes which may lead to tip-over or to inability to climb.

This task is specifically directed at the design and evaluation of a device to detect positive obstacles. The problem of detecting negative obstacles has been deferred while the question of slope detection is taken up under Task D.2.

At the present time, efforts are being directed towards the obstacle detection system concept presented in Ref. 3. In brief, this system takes advantage of the following concept. The sharpness of the image of an object depends on how well focus has been obtained. As the image passes in or out of focus, the light forming the image is either well concentrated or is dispersed. Since non-linear photovoltaic detector will provide an output which is related to the detailed pattern of incident light, it is conceivable that this output can be related to the distance at which the obstacle is located.

Principal areas of activity include: a survey of the types of terrain likely to be encountered on Mars; a study of the optical requirements of the system; an investigation into the detecting capabilities of various sensors; design of suitable electro-mechanical aiming and focusing mechanisms; and development of electronic circuitry to interpret system signals according to simple algorithms and to generate vehicle steering commands.

A terrain modeling table, having one transparent wall, has been constructed. Several topographical photographs have been taken with an f 1.4 50 mm single-lens reflex camera. These photographs, taken at close range (18"-40") with full lens opening, have a very shallow depth of field (DOF) and serve to illustrate an optical method of range determination. The range of an object in the scene is found by passing the plane of focus through the object and noting the range on the camera's focusing ring. White marble sand and some rocks have been principly used as topography in these photographs. Albedo variation, in the future, will be accomplished by mixing several types of sand. Illumination for the scene was provided by a 2000 watt silicon controlled rectifier (SCR) controllable elliptical spotlight which emits a parallel beam similar to that of the sun. The terrain table will, in the future, be used to test out actual system configurations.

The initial system concept as proposed in Reference 3 featured a stationary lens and an electronically scannable vibrating photocell array. In order for this concept to be practical, the system must be capable of analyzing at least a 60 degree azimuth angle while maintaining a shallow DOF to distances of perhaps twenty feet. If it is assumed that both the image size and the array size are to be five inches then, according to the relationship, Ref. 16:

Angle of view (AOV) in degrees = 4 $\tan^{-1}(a/2f)$ where a = image size and f = focal length and the maximum focal length is 9.35 inches. At this point it is necessary to decide on a shallowness of DOF and some measure of defocusing required by the sensors. A two-foot DOF at a distance of twenty feet would appear to be a reasonable figure.

Defocusing can be measured by the size of the circle of confusion, i.e. the diameter of the disk formed by a defocused point source. Here a realistic figure is taken to be 1/32 inch based on focusing experiments with cadmium sulphide (CdS) photocells.

If the foregoing data is substituted into the following relationship, Reference 16,

$$u = \frac{DUF}{DF - d(U + F)} - \frac{DUF}{DF + d(U - F)}$$

F = focal length

d = diameter of circle of confusion

u = depth of field (DOF)

U = distance to object

D = diameter of lens

the result is a diameter of 16.13 inches for a simple lens, (see Fig. 16). This size does not appear to be practical and indicates the need for the consideration of alternate approaches such as scanning.

If the lens diameter must be reduced and with all other factors remaining fixed, it follows that the AOV must be reduced. It has been suggested that if the optical system must be aimed in some manner, it would be prudent to restrict the AOV to such a degree that only one photocell would be required for focus detection.

Clearly it would be cumbersome to physically aim the entire system. The same effect is attainable, however, by other means. It can readily be seen that a gimballed mirror mounted in front of a stationary optical system can produce a scan of a wide area while affording a minimal moving mass. Figure 17 shows one possible arrangement involving a vertically mounted optical system with a periscope type of structure. An inherent advantage of this

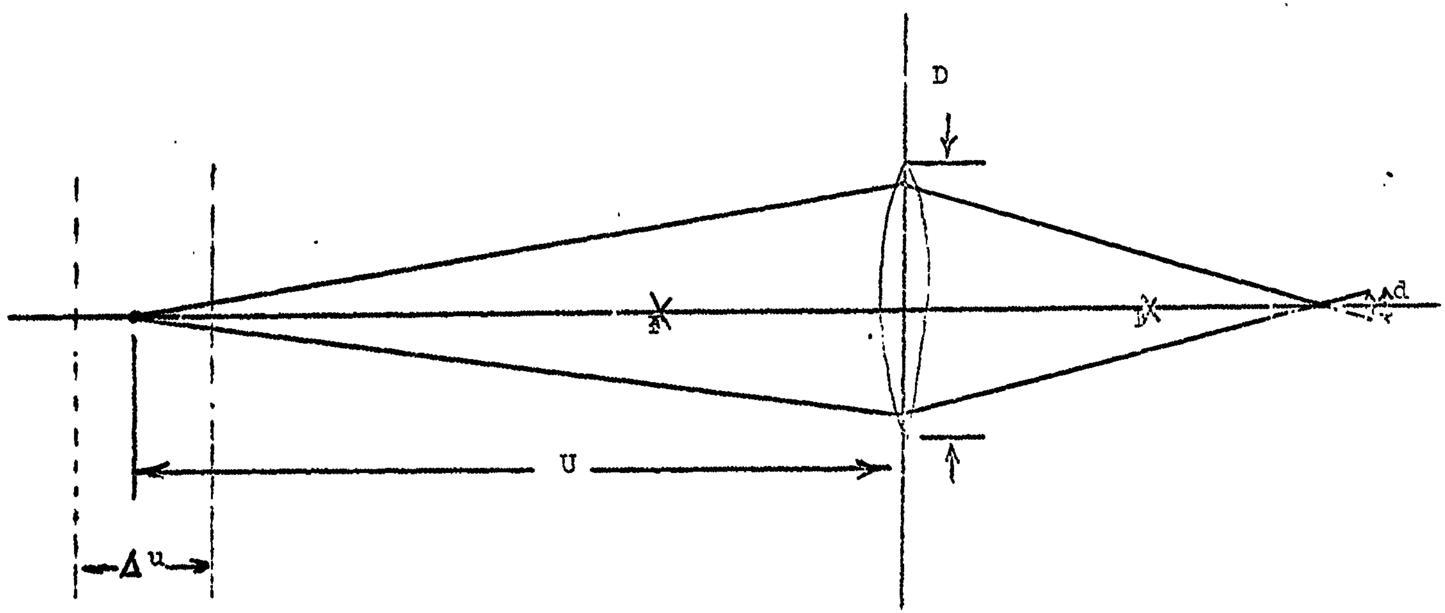

F = focal length

U = distance to object

d = diameter of circle of confusion

D = diameter of lens

Δu = depth of field (DOF)

$$\Delta u = \frac{DUF}{DF - d(U+F)} - \frac{DUF}{DF + d(U-F)}$$

Figure 16. The Geometry Associated with Depth of Field.

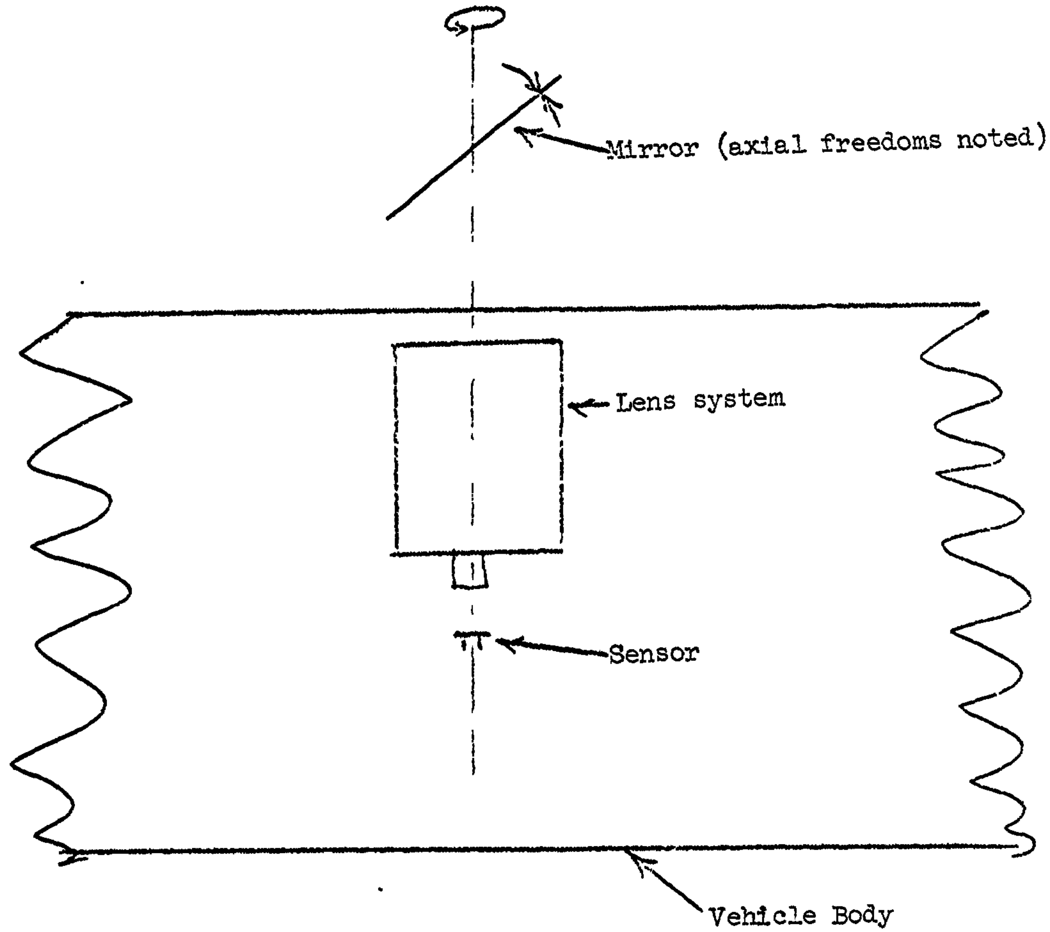
Mirror (axial freedoms noted)
Lens system
Sensor
Vehicle Body

Figure 17

configuration is the possibility of system operation in the event the vehicle must reverse its direction of travel.

The investigation of photocells has thus far yielded the following results:

1. The only suitable materials for the sensors appear to be cadmium sulphide (CdS) and cadmium selinide (CdSe) films. The family of galium arsenide and silicon cells have experimentally been eliminated due to poor focus detecting and relative insensitivity. CdS and CdSe cells exhibit acceptable focus detecting, high sensitivity (on the order of 1/100 footcandle) and slow response as compared to their semiconductor counterparts.

2. The CdS and CdSe cells can detect the focusing of a point or line source of light on their surfaces. Simple bar and dot images have also yielded observable results for various cells. At the present time, however, no continuous tone images have met with success. Several hypotheses have been considered to explain the successes and failures. None, as yet, can explain all effects.

At the present time, three types of focusing mechanisms are being considered. They are: (1) moving the lens; (2) moving the sensor; (3) moving an intermediate mirror.

The first system has the advantage of being accomplished by rotary motion alone. This allows for a rigid structure that is very vibration resistant. Its principal disadvantage is that it involves the motion of the relatively massive lens system.

The second scheme has the advantage of being light in weight and still affording reasonable structural rigidity. The motion, however, would involve the stressing of delicate electrical connections and could precipitate a system failure.

The third system is free of electrical connections and is relatively light in weight, but is complicated in nature and apt to be fragile.

Questions relating to electronic circuitry are so dependent on the structure of the other parts of the system that this phase must be deferred until a proper base has been developed.

The present emphasis is being placed on the photocell investigation. It is felt that the success or failure of the entire system, as presently conceived, hinges on the focus detecting ability of these cells when presented with images of realistic scenes. The major part of the effort in the immediate future will be devoted to obtaining a better understanding of the focus detecting ability and its limitations. If the detection concept is proved to be feasible, efforts to implement it will then be undertaken.

Task D. Vehicle Dynamics and Attitude Control

Task D.1. Dynamics of a Two-Segment Vehicle - J.A. Hudock
Faculty Advisor: Prof. E.J. Smith

The Mars roving vehicle will require some form of attitude control. This statement can be justified by considering the tasks which the vehicle is required to perform. These tasks fall under two categories; those which are performed while the vehicle is stationary, and those which are performed while the vehicle is in motion. The first category is not under major consideration currently in this project.

The second group of tasks can further be subdivided into tasks which need an exact orientation of the vehicle or instruments and tasks which need only a general vehicle position. Maintaining the vehicle within the required orientation for all tasks can demand overly excessive power and hardware requirements. Therefore, the attitude control of those instruments requiring a more precise orientation can best be provided, with regard to weight and power limitations, by an individual attitude control of the instruments requiring it.

A more general suspension system for the entire vehicle is desirable to reduce the effects of shock and impulse forces, acting in the contact points of the vehicle with the surface, as the vehicle travels across the planet. This suspension system can be provided by a passive system to reduce power and space requirements of the vehicle.

Preliminary work on a passive suspension system for a one segment vehicle, Ref. 3, was primarily concerned with induced oscillations due to coupling between channels in a three-degree of freedom model. The two-segment vehicle currently under consideration has two advantages over a single segment vehicle. First, it is more capable of a stable orientation while stationary due to a flexible coupling between segments. Second, the use of a flexible coupling may provide a means of reducing shock and impulse forces on the near segment and reduce the higher frequency components of oscillations experienced by the rear segment.

The preliminary general vehicle model, Fig. 18, is composed of two rectangular segments connected with a flexible rod. Each segment is mounted on a visco-elastic axle for suspension, modeled as a combination of parallel springs and dashpots. The choice of visco-elastic axles over other forms of suspension is promoted by a desire for a less massive configuration than individual springs and shock absorbers. The techniques involved in the analysis can also be extended to other forms of suspension.

The preliminary vehicle model has three degrees of freedom: heave, or vertical motion of each segment; pitch, or rotation about an axis perpendicular to the direction of vehicle travel; and roll, or rotation about an axis parallel to the direction of travel. This model does not take into account lateral motion and furthermore the surface is assumed to act with only upward components on the vehicle suspension points.

The equations of motion have been written for this model for the heave, pitch, and roll motions. The equations are made with several assumptions:

1. Transforming from the body fixed axis, which is assumed to coincide with the geometric center of each segment, to the inertial axis fixed on the surface, the angular motion is assumed small enough to consider the sine of an angle equal to the angle and the cosine of an angle equal to unity.

2. The body fixed angular velocities are small enough so their products can be neglected.

3. The mass of connecting rod and wheel dynamics are neglected.

4. The suspension legs remain parallel to the vertical inertial axis and have no lateral motion.

The choice of vehicle geometry and segment masses were chosen to follow the same general size and weight of the model studied in Ref. 3. The suspension constants are to be varied to determine a general outline of vehicle performance as a function of the suspension constants. This

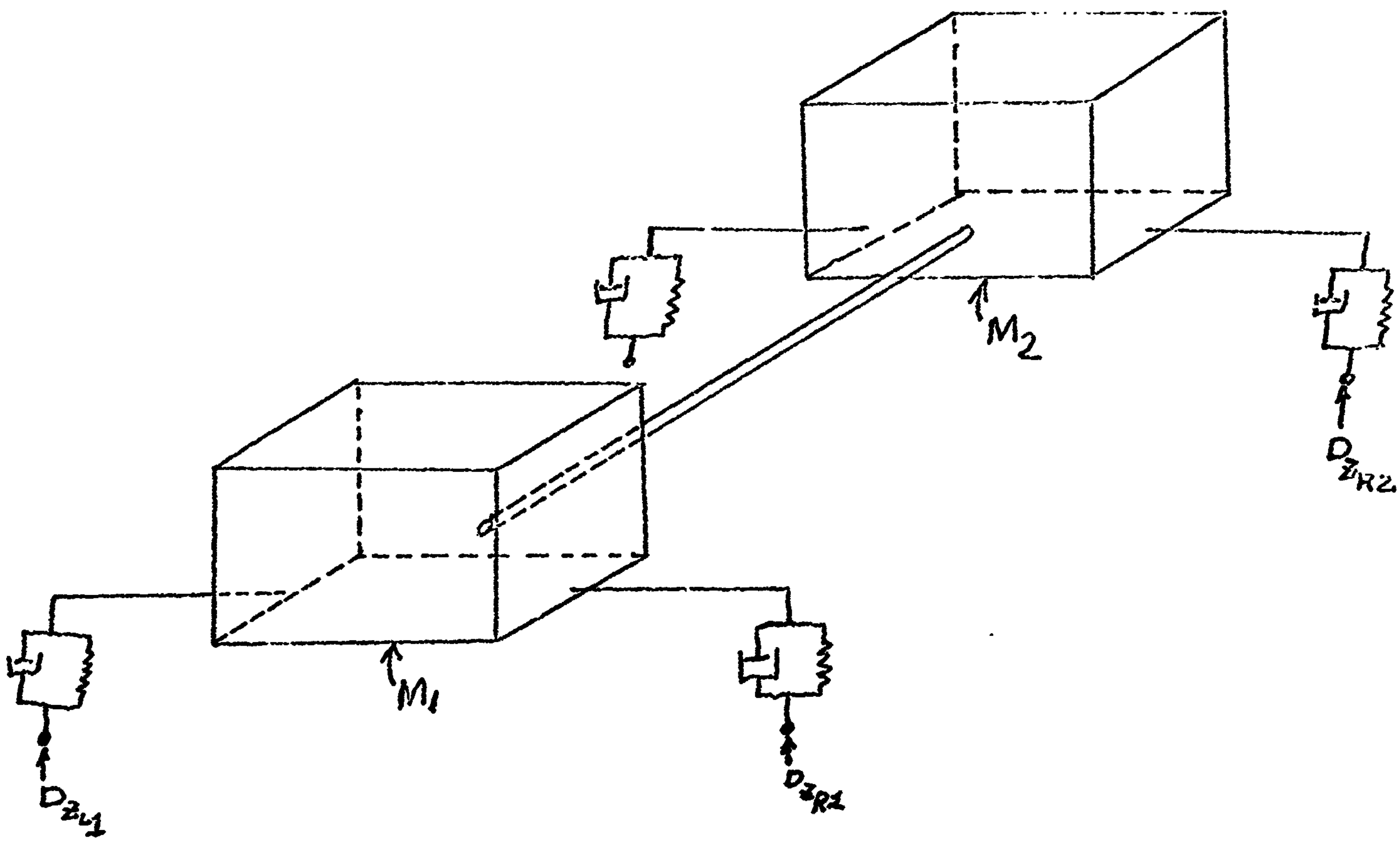

Figure 18. Two-Segmented Vehicle

be accomplished by an analog simulation of the equations to determine vehicle response to shock and impulse forces as well as induced oscillations.

An analysis of the root-locus plots for the linear equations of motion will be made to determine the effects of system parameters on vehicle response. More detailed work in this area lead to establishing a set of criteria for suspension parameters to provide an optimal passive attitude control system for various vehicle configurations. Work in this area will depend primarily upon a further knowledge of other on-board systems and their requirements regarding shock and vibration. The analysis of a passive suspension system has therefore been as general as is practicable, with regard to obtaining meaningful results, to date due to the limited amount of information on overall system requirements.

Further work will center about derivation of more exact non-linear equations which will eliminate as many of the assumptions in the linear model as possible without making them unnecessarily complex. These equations will be simulated on a digital computer to evaluate vehicle response.

Once the on-board systems and their shock and vibration limits are defined, practical design guidelines relating to design of the vehicle and its suspension system should be forthcoming.

Task D.2. Attitude Detector Systems - A. Himmel, J. Jendro, J. Mleziva and N. Pinchuck
Faculty Advisor: Prof. E.J. Smith

The attitude detector system on a roving vehicle is required to fulfill several functions. First, while the vehicle is stationary, to provide the information required by an attitude control system to bring the vehicle or some component of it to a specified attitude for purposes of experimentation or terrain sensing. Second, while the vehicle is in motion, to provide information required for the interpretation of obstacle detectors, note Task C.2., and to provide information as to the slope of the terrain in terms of pitch and roll as it relates to the vehicle. Third, depending on the devices used for attitude detection, these systems may be combined with additional sensors to provide navigational data.

The attitude detection system for the martian vehicle poses two challenging problems. The first deals with the derivation of Euler angles from attitude sensor measured angles or angular rates. The second problem deals with the dynamics at the sensors themselves.

An example of the first problem would be detecting vehicle attitude by means of a two-degree-of-freedom gyro. Electrical pickoffs can be used to detect the motion of the gimbals. These measured gimbal angles must be related to the vehicle attitude with respect to inertial space. If a vertical gyro is used, the vehicle is free to turn about the gyro spin axis. This motion cannot be detected by the gimbals. Another device must therefore be used to detect this motion. However even if the vehicle turning motion in azimuth is detected, the vehicle attitude cannot be determined without ambiguity. One method that can be used to determine attitude without ambiguity is to use a known mathematical rotational transformation that can specify vehicle motion, with respect to inertial space, from one orientation to another. Euler angle transformations are one of several methods that can be used to solve this problem. However the difficulty arises when an attempt is made to relate gimbal angles to Euler angles. This remains an unsolved problem that is currently under study.

The second problem deals with the ability of an attitude sensor to faithfully reproduce the attitude of the vehicle as it jolted and bounced by its motion over the surface. The sensor must have sufficient speed of response to accurately react to the dynamic motion of the vehicle but still not introduce an error due to accelerations of the sensor. (i.e. motion of a pendulum sensors pivot point).

These two problems are currently under study with the emphasis being currently placed on the resolution of measured angles into Euler angles, a problem is common to all sensor configurations. Another area under investigation is it relates to the use of redundant sensors to eliminate ambiguities.

Four sensor devices are now under study: single-degree of freedom pendulum, two-degrees of freedom pendulum (preliminary concepts are summarized below, Task D.2.a.), two-degrees of freedom gyroscope, and rate gyroscope. It is expected that the problems of relating the measurable quantities unambiguously to attitude for each type of sensor will be resolved by March 15. Specification of configuration and analysis of dynamic response for each type of sensor should be obtained by May 30.

Task D.2.a. Design of an Attitude Sensing Pendulum -
J.M. Mleziva
Faculty Advisor: Prof. E.J. Smith

Included in the main problem of determining a verticle (or horizon) for the vehicle are two "sub-problems".

The first problem is one of resolving the pendulum outputs (which are angles) into Euler angles, was discussed under Task D.2. above.

The second problem is to design a suitable pendulum and to adjust the parameters to give accuracy required under stationary as well as dynamic conditions. This problem is being systematically approached as follows:

1. Investigate different configurations

2. Observe dynamics and adjust parameters in:

   a. one dimensional analysis
   b. two dimensional analysis

3. Procurement and testing of components for use in construction

4. Analog computer simulation and/or construction

The first configuration, Fig. 19, was chosen because of its simplicity. It centers around a gimballed pendulum, free to move (except for possible damping forces) about two axes. The angles between the gimbal axes and the pendulum bob represent the measurable quantities which must be used to determine attitude. Again, looking for simplicity and reliability, a simple variable resistor or similar device can be used for angle measurement.

The material requirements would include:

4 bearings (roller, jewel, or other)

1 circular support, possibly elastic

1 elastic straight support

2 sensors; one of which may be a magnetic pick-off to achieve greater accuracy, the other probably a simple potentiometer.

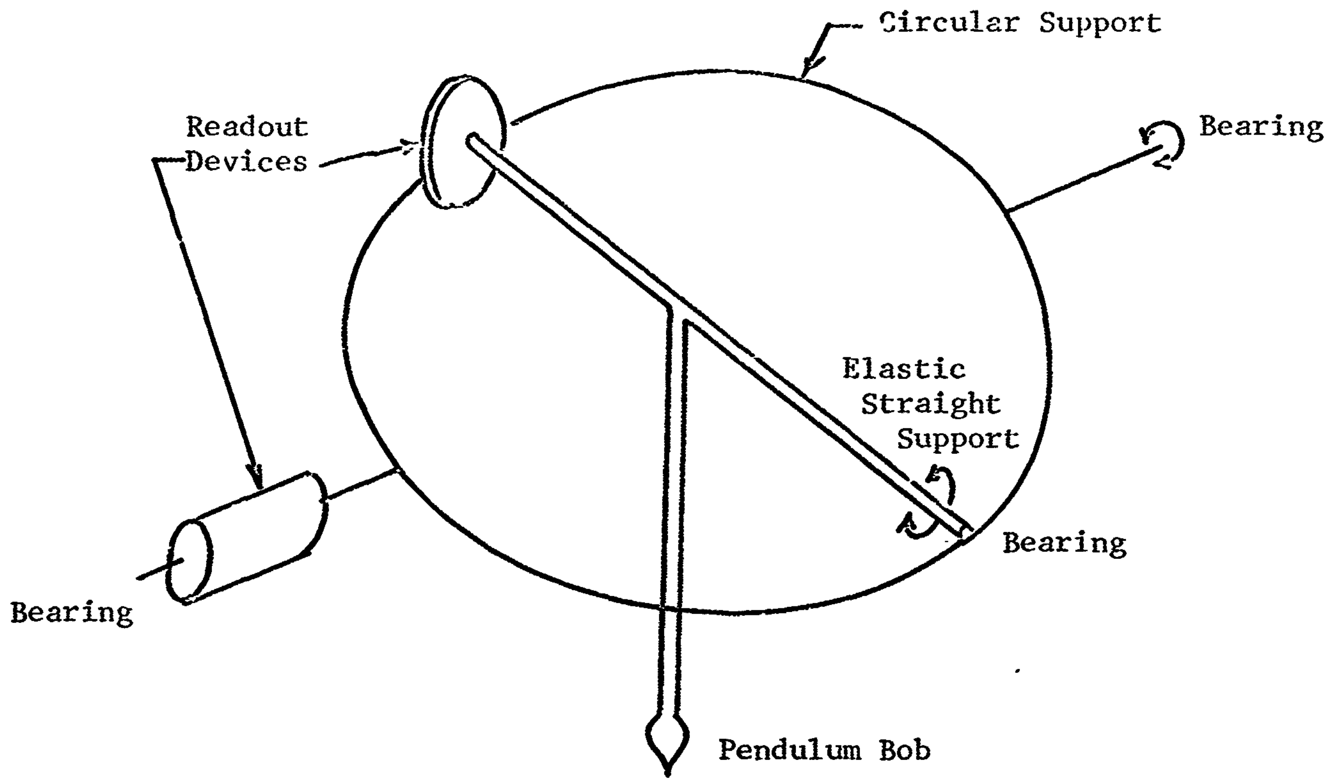

Figure 19. Conceptual Design of Attitude Sensor

There are certain problems associated with this configuration. One of the limitations is inherent in the readout devices. Since one of them is mounted on the support, it must be light in weight so as not break the structure during the takeoff/landing phase. Since the accuracy of the readout is limited only by the nature of the device; there is no way to improve accuracy if it is not satisfactory. Another of the limitations is the force and vibration the readout devices will withstand before they themselves cease to function. A common potentiometer was tested (axial loading) to more than 50 lb-f before destruction, but this is still none to much leeway.

The advantages of this configuration include the fact that if the axes are arranged correctly within the vehicle, the outputs need no conversion to that coordinate system, cutting our transformation problems in half (only one transformation instead of two).

The second design configuration was considered to correct one of the chief disadvantages of the first, namely the fact that the inherent accuracy is limited by the readout devices. The second configuration again suspends a free swinging pendulum but the readout is to be taken at the end of the pendulum. By determining the position of the pendulum bob, the orientation of the vehicle can be computed. In order to determine the position of the pendulum, a current flows through the structure, down the pendulum, and to one of many wires imbedded in a "dish". By sensing which wire the bob is in contact, the position is determined. This configuration can be made as accurate as desirable since the length of the pendulum can simply be increased until satisfactory. Two pendulums are required, but if a small computer were used it would be possible only with one.

The disadvantages of this configuration are first, the size may be prohibitive; second, the support would have to support more weight and carry current; and third, the roll and pitch angles have to be calculated.

Somewhat arbitrarily, but primarily for the sake of simplicity in the time allotted for this project, the first configuration was chosen in the hope that the accuracy would be sufficient for our purposes.

Preliminary testing of components showed that if the structure could be expected to withhold 50 lbs or so; (as indicated by the potentiometer) the weight of the pendulum bob would have to be no larger than the neighborhood of 10's of grams, (in order to withstand 50 g accelerations).

This may or may not be enough to actuate the pendulum and therefore a design with minimal friction is desirable.

The second portion of this project is the analysis of pendulum dynamics, so that the damping, mass, and length parameters may be determined for simulated conditions.

The procedure followed in this process is the progression from the simplest case to the most complex, in the expectation that the simpler problems will yield insight into the more difficult ones.

The problem is made more complex if small angle approximations cannot be made. Since the vehicle is designed to climb a 30° slope, the pendulum must be accurate to at least 30°. The error in the linear approximation $\theta = \sin\theta$ at $\theta = 30^{\circ}$ is $\frac{.500 - .478}{.500}$ or 4.4%. Also a moderate jolt could easily cause very large angles to be attained. Since an accuracy of the order of one degree is desired, the non-linear formulations must be used.

Task E. Chromatographic Systems Analysis

One important phase of the initial Voyager missions to Mars is the search for organic matter and living organisms on the martian surface. The present concept for attaining this objective consists of subjecting samples of the atmosphere and surface matter to certain chemical and biologically related reactions and thereafter analyzing the products produced. The most likely system for a general chemical analysis appears to be a combination gas chromatograph/mass spectrometer. This unit would be a major component in the biological and chemical laboratory of an unmanned, remotely controlled roving lander for Mars. It is the objective of this task to generate fundamental engineering design techniques and system concepts for use in optimizing the design of such a chromatograph separation system. Such a system should provide maximum resolution with minimum retention times and minimum carrier gas usage and should be capable of separating components evolving from many different kinds of experiments.

Because of the variety of the mixtures to be separated and the complexity of the fractionating process, a system analysis based on the mathematical simulation of the chromatograph is being undertaken. This technique will use mathematical models, which will incorporate fundamental parameters evaluated from reported experiments, to explore various concepts and to direct further experimental research.

A first order mathematical model of chromatographic column was developed. The model was compared to actual chromatographic data, and was able to predict the retention time of the sample but failed significantly in predicting peak spreading, Ref. 3 and 17. Because a reasonably accurate model is required for system evaluations, new studies are now being undertaken. It is believed that the spreading may be attributed to either diffusional effects neglected in the first order model or to imperfect injection of the samples.

These problems are being attacked by a three-member team, each of whom is pursuing specific assignments:

1. The mathematical model is being improved by considering second order terms related to diffusion. Because of the difficulty in obtaining time-domain solutions to the equation, the method of moments is being pursued.

2. Reliable methods for predicting system parameters are being sought. Prior work in general is not applicable because new systems are an order of magnitude smaller than commercial equipment. Some recently reported research offers promise.

3. The approximate effect of finite injection time for the sample upon the chromatograph is being studied theoretically using the previously developed first order model. Approximate limitations on system performance will result from this study. An experimental test system to evaluate the models and system concepts is being constructed.

It is expected that by June 1969, the performance of a chromatograph can be predicted well enough for system studies to commence. The testing equipment should also be operable at that time.

A mathematical model of the chromatographic column, based on the unsteady state mass transport of a single chemical species in a carrier gas/adsorbent system was derived earlier, Ref. 17. This model consisted of the following system of dimensionless equations:

$$\frac{\partial y}{\partial \Theta} = -\frac{1}{1-y}\left(\frac{\partial y}{\partial z}\right) + \frac{1}{Pe}\left(\frac{\partial^2 y}{\partial z^2}\right) - N_{tOG}\,(y-y^*) \qquad \text{(gas phase)}$$

$$\frac{1}{R_o}\,\frac{\partial x_L}{\partial \Theta} = N_{tOG}\,(y-y^*) \qquad \text{(adsorbent phase)}$$

$y^* = m\, x_L$ (adsorption thermodynamics)

in which

- y = gas composition
- y^* = composition of gas in equilibrium with adsorbent phase
- z = position in column
- θ = time
- x_L = composition in adsorbent phase
- R_o = gas/adsorbent ratio
- m = adsorption constant
- N_{tOG}, Pe = column parameters

The second derivative appearing in the gas phase equation represents gaseous diffusion of the adsorbing compound in the direction of carrier gas flow. In many cases, especially when the diameter/length ratio of the column is small, this term is not of prime importance. For exploratory studies, this term was neglected and only the first order effects were studied. Solution of the simplified equation set (1) resulted in the following:

$$y(\theta, z) = 0 \quad \text{for } \theta < z$$

$$y(\theta, z) = \frac{N(v/L)}{w} \exp\left[-N_{tOG}\right] \exp\left[\frac{-(\theta - z)}{T}\right] \cdot \left[\frac{2N_{tOG}z}{\tau} \cdot \frac{I_1(x)}{x} + \delta(\theta - z)\right] \quad \text{for } \theta > z$$

in which

- I_1 = modified Bessel function of the first kind, of order one
- L = length of column
- N = sample size
- v = carrier gas velocity
- w = carrier gas flow
- δ = Dirac delta function
- τ = $N_{tOG}\, mR_o$
- x = $2\left(\frac{N_{tOG}z(\theta - z)}{\tau}\right)^{1/2}$

This solution assumed that the time for sample injection was negligible compared to the times involved in the process (an impulse).

To evaluate the adequacy of the model, the theoretical and experimental chromatograms for pentane were compared, Fig. 20.

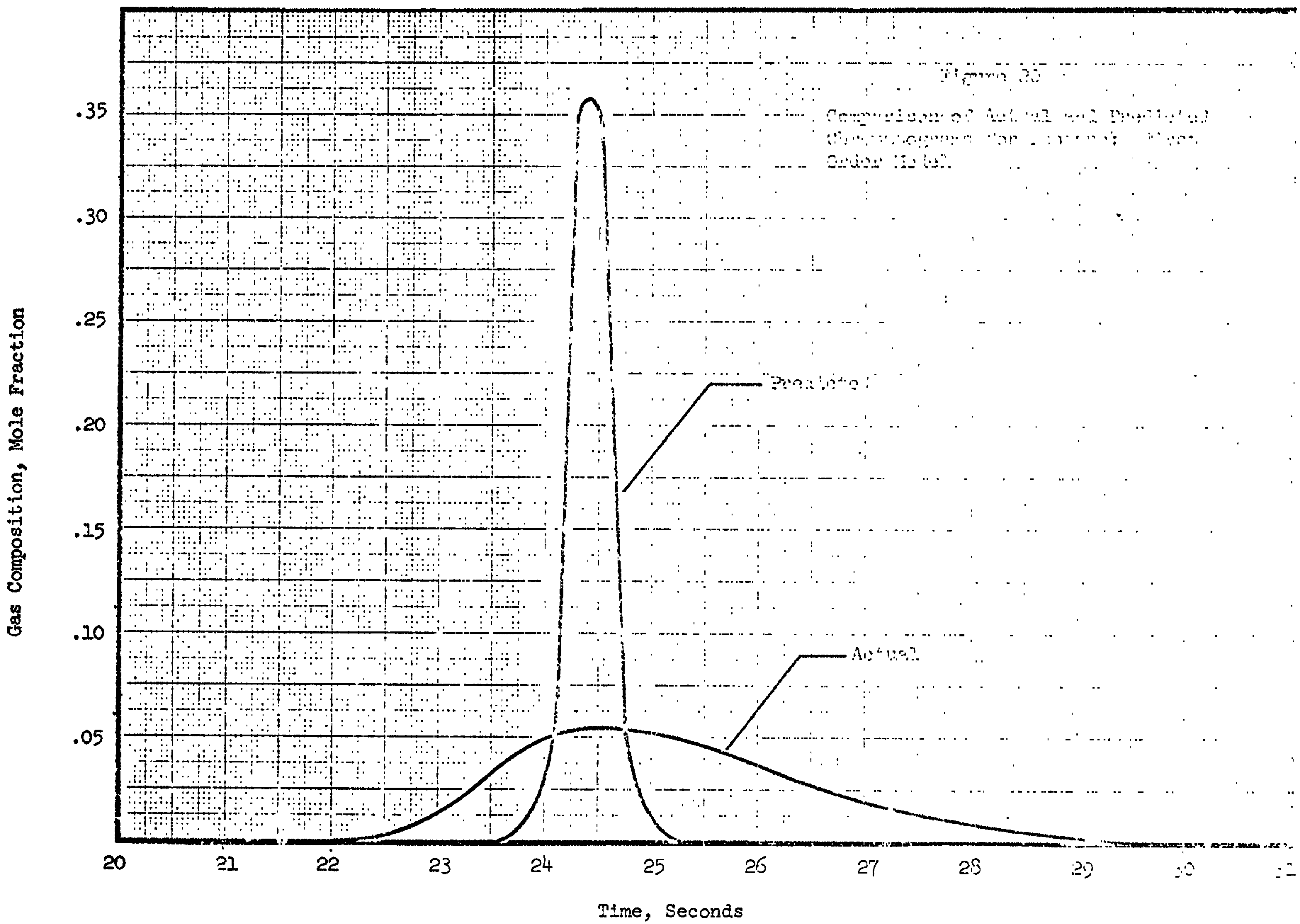
Gas Composition, Mole Fraction
.35
.30
.25
.20
.15
.10
.05
20
21
22
23
24
25
26
27
28
29
Time, Seconds

The model exhibits the basic characteristics of the experimental data, although it fails significantly in predicting peak spreading. Because a reasonably accurate model is required for system evaluations, additional studies are being undertaken.

It is believed that the spreading may be caused by two factors:

1. Diffusional effects associated with the neglected second order term in the gas phase equation.

2. Actual sample injection was not adequately represented by an impulse.

These problems are being attacked by a three-man team, each of whom is pursuing a specific assignment:

1. Improvement of the mathematical model by considering the second order term.

2. Development of methods for predicting the column parameters which appear as constants in the system equations.

3. Investigation of the effect of sample injection time upon the resulting chromatogram.

Task E.1. Second Order Model Analysis - W.A. Voytus
Faculty Advisor: Prof. P.K. Lashmet

Work under this task has been devoted to the development of a mathematical model which adequately describes the behavior of the gas chromatograph. It appears that at the low gas flow rates that are anticipated in columns suitable for a space voyager, the longitudinal mass diffusion in the column begins to approach the rate of transport due to bulk flow of the carrier gas. Since this longitudinal transport is related to the Peclet number, Pe, the complete system of equations presented earlier must be solved.

To estimate the effect of the second order term containing the Peclet number, the equations were solved for the limiting case of equilibrium adsorption. Mathematically this implied that

$$N_{tOG} \rightarrow \infty$$

$$(y - y^*) \rightarrow 0$$

or the column was very long and very efficient. The effect of several values of the Peclet number on the output of the chromatograph column is shown in Fig. 21. Clearly, there are conditions under which diffusion can seriously affect the performance of the column.

Solution of the system equations requires four boundary and initial value conditions. Three of these are somewhat obvious:

1. Concentration of the component in the gas is initially zero.

2. Concentration of the component in the adsorbent is initially zero.

3. The sample injection can be specified as a function of time.

However, the fourth condition involves an intuitive approach to the system. Danckwerts, Ref. 18 has proposed

$$\partial y/\partial z = 0 \qquad (L = \infty)$$

and Wehner and Wilhelm, Ref. 19 have suggested that y is finite ($L=\infty$). The validity of these conditions for some finite length column is not as obvious as authors would have us believe. The effect of the analysis detectors at the rear of the column, which may or may not be significant, is neglected, for instance. However, because it appears that the specific boundary condition has little practical effect upon the numerical results, Ref. 20, the equations are being solved using the above conditions.

The solution of the equations themselves presents a formidable task. A time domain solution to the system equations has yet to be found. Work recently, has been directed to obtaining information from the solution in the Laplace-transform (or other transform) domain. This work involves statistical moments, theoretical values of which can be obtained from the transform domain solutions, Ref. 21,22,23,24. Kucers, Ref. 21, has proposed a time-domain solution composed of an infinite series of Hermite polynomials, the coefficients of which can be computed from these moments. Grubner, Ref. 22,23, has attempted to relate the moments to experimental data, but the results are somewhat qualitative.

At the present time, it appears that use of the moments offers the most fruitful approach to the time behavior analysis. This involves extension of the previous

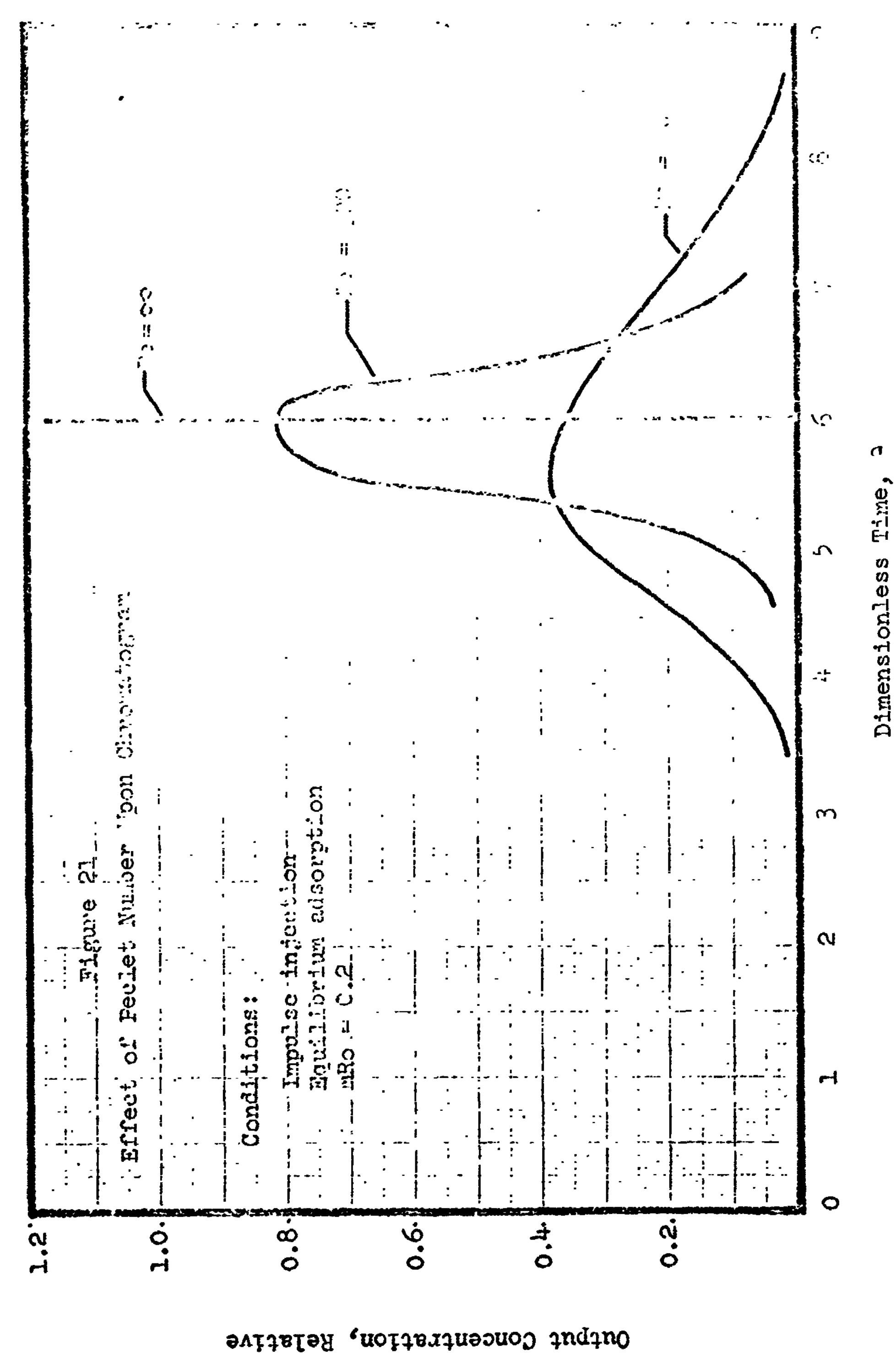
Figure 21
Effect of Peclet Number Upon Chromatogram
Conditions:
Impulse injection
Equilibrium adsorption
mRo = 0.2
Output Concentration, Relative
Dimensionless Time, θ
1.2
1.0
0.8
0.6
0.4
0.2
0
1
2
3
4
5
6

work by quantitatively relating the theoretical moments, which are functions only of the column parameters (Peclet number, gas flow rate, column length, etc.), to peak height, peak spreading, and tailing.

Task E.2. Transport Parameter Estimation - D.A. Reichman
Faculty Advisor: Prof. P.K. Lashmet

When the development of the second order model of a chromatographic separator discussed above has been completed, the usefulness of the final equation will depend upon the availability of methods for estimating the model parameters. One parameter of the second order model is the Peclet number, Pe. This dimensionless number is a measure of axial dispersion or mixing in a chromatographic column. If the axial dispersion were assumed zero, the Peclet number would be infinite and the model would reduce to the first order representation developed in the prior work, Ref. 17. It is the objective of this task to develop a suitably accurate method for the estimation of the Peclet number.

A literature search has been conducted in an attempt to find either compilations of data or existing correlations for the Peclet number. Several independent correlations in good agreement with each other have been found. These include those by Wilhelm, Ref. 25, Bischoff, Ref. 26, and Hiby, Ref. 27. Unfortunately, the range of gas flow applicable to this project is below the range considered in the literature correlations. The lowest Reynolds number (a dimensionless constant proportional to the gas flow rate and indicative of the fluid mechanics of a system) considered in the literature is about 0.05, with most reliable data falling above Reynolds numbers of 10. The flow range suitable for this project lies below a Reynolds number of 0.05. Figure 22 is a summary of correlations by Wilhelm, Levenspiel and Bischoff, and Hiby, Ref. 27. The Peclet number appears to be linear with Reynolds number at low Reynolds numbers. This is misleading and it must be noted that in this range the curve is a linear extrapolation through a very few data points. Extrapolation of such curves to lower Reynolds number is not advisable since at low flow rates molecular diffusion is believed to contribute significantly to the dispersion process. Also, these correlations ignore complications such as effects of particle shape, particle size, and packing arrangement which may be important at low flow rates. The literature correlations uncovered thus far

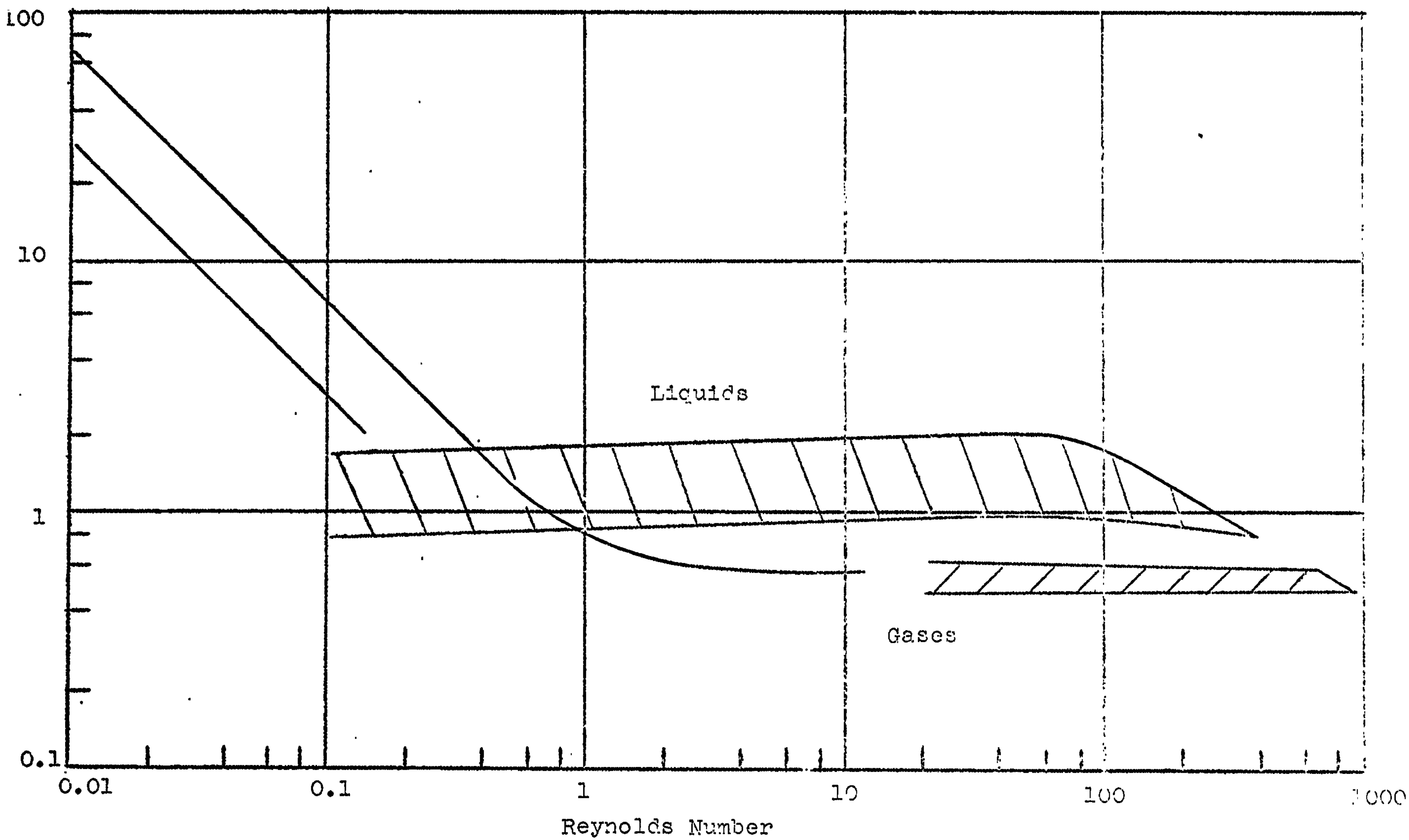

Figure 22. Summary of Available Peclet Number Data

will yield only a gross estimate of the Peclet number which would be inadequate for design purposes. Efforts to find data below a Reynolds number of 0.05 will continue.

Consideration was given to the possibility of using diffusional models with highly simple geometries for the estimation of dispersion. Four such models have been reported, Ref. 29:

1. Random Walk Model: This model postulates that mixing is the result of random deflections of particles.

2. Rest Phase Models: These models assign probabilities of a particle being either in motion in a restriction between elements of packing or at rest in a void space. From this the probability of finding any number of gas particles at a certain position and time may be computed.

3. Turner's First Model: This model views packing as a series of capillaries of equal length and diameter separated by stagnant pockets. All mass transfer into and out of the pockets is by molecular diffusion, and dispersion in the channels is modeled as axial-dispersed plug flow.

4. Turner's Second Model: The packing is viewed as an aggregate of channels of various lengths and diameters with axial-dispersed plug flow in each channel.

In general, the simplicity of the models renders them insensitive to packing parameters and, as with the literature correlations, only order of magnitude results can be obtained.

A more promising approach to the problem of estimating Peclet numbers has been developed by Johnson, Ref. 30, from the work of Taylor, Ref. 29, and Rhodes, Ref. 31. The method compares the second moments of two mathematical models of a chromatographic separator to arrive at an expression which yields the Peclet number as a function of the velocity profile, geometry, and fluid mechanics of the system. The two mathematical models considered are a developed flow diffusional model and a plug flow model. Comparison of the second moments of the two models leads to equations relating the dispersive diffusional coefficients to the various molecular diffusivities and various fluid mechanics factors. These various factors may be estimated from basic studies conducted by others, Ref. 31 and 32. Application of these methods yields a working equation relating the Peclet number to known fluid flow properties, known chemical characteristics of the system, and the physical dimensions of the packing and column. This equation is for uniform packing and must be modified to treat segregated packings usually encountered in practical chromatographs. This method appears promising but its accuracy at low Reynolds numbers and its compatability with the second order model discussed in the previous section are yet to be determined.

One other approach to the estimation of Peclet numbers to be considered in the immediate future is the use of heat and mass transfer analogies to estimate axial dispersion of mass from correlations of heat flow in packed beds.

Task E.3. <u>Sample Injection Problem</u> - R.C. Krum
Faculty Advisor: Prof. P.K. Lashmet

It is the objective of this task to evaluate the techniques for injecting the samples and to determine practical limitations on the system design. The task involves both a theoretical analysis and the development of a system testing facility.

The first-order model of the chromatograph developed previously was studied for an impulse-type injection of the sample. Since an impulse is mechanically impossible as an input to a chromatographic system, part of the task will involve determining the effect of injecting the sample in finite periods of time. Input functions which are mechanically feasible, such as the square and triangular pulses, will be considered with the first order model to determine the effect these functions have on output resolution.

To obtain an estimate of the effect of finite injection time upon column performance, the first order model is being considered using a square pulse instead of the impulse as the injection. In performing this analysis, the following integral was encountered:

$$\int_0^{\theta} \frac{\exp(-\lambda) \cdot I_1(x)}{x} d\lambda$$

in which

$$x = 2N_{tOG}\sqrt{mR_o z\lambda}$$

Initial attempts to evaluate this integral analytically failed, and a numerical analysis is now being applied. Numerical integration by Simpson's technique is being used and the Bessel function is being expanded in an asymptotic form. In order to determine the exact effect sample injection has on the first order model, the argument values in the preparation of Fig. 22 are being used in this study. Because of the extremely large values of some of these arguments, computational difficulties have been experienced. The computational schemes have been reprogrammed and the problems appear to be solved.

The second part of the task concerns the construction of a gas chromatographic test system. The system will be flexible enough to permit the testing of various sized columns. A Perkin-Elmer, Model 154-C, chromatograph is being renovated and revised for this purpose. Input and output detectors having time constants of the order of 0.04 seconds will be installed. These small detectors, which will be required in the envisioned space voyage, represent an appreciable improvement over the normally available detectors (0.5 second time constant). The proposed system will permit accurate, fast monitoring of both the input and output signals of the chromatograph by a light beam galvanometer, which is compatible with the small time constants of the detectors, so injection techniques can be evaluated. Eventually the test system can be used for evaluating the chromatograph models and system concepts.

It is the objective of these current efforts in this overall task to produce the following by June 1969:

1. A working mathematical model which represents the behavior of the chromatograph column.

2. Reliable methods for predicting the physical parameters of the system.

3. An understanding of the effects of finite sample injection time and the limits it imposes upon the separating ability of the column.

4. An experimental testing system for evaluating the model and system concepts.

5. Possible initial evaluation of some system concepts.

Work after the completion of these efforts will involve the evaluation of the effectiveness of system configurations in separating complex gas mixtures and the development of design methods for maximizing system performance under space voyage conditions.

IV. Educational Considerations

In addition to the technical goals outlined earlier, this project has the objective of promoting the education of engineering students in directions and dimensions not normally encountered in formal programs of study. In brief, the project activity provides real problems of substance whose solution is obtained not by the application of expedient simplifications to make them manageable but rather according to the technical needs that realistically apply to the situation. Accordingly, the students learn to accommodate to trade-offs be een competing values and to work with boundary conditions and constraints originating with the factual situation and which may be compounded by the interfacing of tasks. In this type of environment, the student perceives that his role in professional practice will normally involve a significant amount of interaction with other individuals and that his work cannot proceed independently and without consideration of and impingement by the work of others. Furthermore, he is forced to obtain, understand and utilize knowledge which is on occasion far removed from his own speciality field and to undertake research when necessary to obtain the required information. Although the very nature of the problems and the faculty perspective emphasize the relevance and importance of the technical goals, the periodic visits of Mr. Eric Suggs of the Jet Propulsion, and on occasion of other NASA representatives, to review progress reinforce these concepts dramatically.

From an educational point of view, the project has proven to be an unqualified success. Large numbers of students (approximately 40 in two years) have had the unique experiences of real-life involvement in engineering problems within the context of their formal education.

Pertinent information regarding the participating students, their degree goals or achievements, the period of participation and their support relationship to the project is summarized below. While this information may be of general interest, its primary value insofar as this progress report is concerned is that it provides a basis for evaluation of the progress made in individual task areas. It should be noted that all students are meeting an academic requirement by this activity.

The following students met their degree requirements since July 1, 1968:

P. Cefola,	7/1/67-11/30/68	Ph.D. (Mech.Eng.)	Proj.Stipend & Tuition
R. Janosko,	7/1/67- 1/30/69	M.Eng. (Mech.Eng.)	Proj.Stipend & Tuition
T. Sliva,	2/1/68- 8/30/68	M.Eng. (Chem.Eng.)	Self-Supported

The following students are seeking degree goals and have had project support during the next academic term:

L.Hedge	9/1/68-	M.Eng.	(Mech.Eng.)
R.Janosko	7/1/67-	Ph.D.	(Mech.Eng.)
J.LaBarbera	9/30/68-	M.Eng.	(Elec.Eng.)
R.Mancini	9/15/68-	M.Eng.	(Elec.Eng.)
J.Morgan	9/30/68-	B.S.	(Mech.Eng.)
D.Reichman	9/15/68-	M.Eng.	(Chem.Eng.)

The following students have been participating in the project without project support but will be receiving stipend and tuition support from the project during the coming academic term:

J.Hudock	9/15/68-	M.Eng.	(Elec.Eng.)
P.Rayfield*	7/ 1/68-	Ph.D.	(Mech.Eng.)

The following students are participating in the project to meet their academic engineering project or thesis requirement and have not received financial support* from the project.

R.Carron	9/15/68-	M.Eng.	(Mech.Eng.)	Cluett-P. Fellowship
A.Himmel	9/15/68-	M.Eng.	(Elec.Eng.)	NSF Fellowship
J.Jendro	9/15/68-	M.Eng.	(Elec.Eng.)	NSF Fellowship
T.Kershaw*	7/ 1/67-	Ph.D.	(Mech.Eng.)	NDEA Fellowship
R.Krum	9/15/68-	M.Eng.	(Chem.Eng.)	DuPont Traineeship
J.Lazzara	11/ 1/68-	M.Eng.	(Mech.Eng.)	Teaching Assistant
J.Mleziva	9/15/68-	M.Eng.	(Elec.Eng.)	Teaching Assistant
N.Pinchuck	9/15/68-	M.Eng.	(Elec.Eng.)	Teaching Assistant
J.Sadler	9/15/68-	M.Eng.	(Mech.Eng.)	Teaching Assistant
W.Voytus	9/15/68-	M.Eng.	(Chem.Eng.)	NSF Fellowship
R.Wepner	9/15/68-	M.Eng.	(Mech.Eng.)	NASA Fellowship

* Mr. Kershaw and Mr. Rayfield received partial support from the project during the summer of 1968.

References

1. Shen, C.N. and P.J. Cefola, "Adaptive Trajectory Control for Mars Entry Based on Sensitivity Analysis", AIAA 68-835, Presented at the AIAA Guidance, Control and Flight Dynamics Conference, Pasadena, Calif., August 1968.

2. Janosko, R.E., "On-Line Parameter Updating of the Martian Atmosphere with Minimum Storage, R.P.I. Technical Report MP-2, Rensselaer Polytechnic Institute, Troy, N.Y. January 1968.

3. Lashmet, P.K., I. Lee, G.N. Sandor, C.N. Shen, E.J. Smith and S. Yerazunis, "Analysis and Design of a Capsule Landing System and Surface Vehicle Control System for Mars Exploration," Progress Report, Jan. 1, 1968 to June 30, 1968, Rensselaer Polytechnic Institute, Troy, N.Y., June 1968.

4. Levine, G.M., D.E. Evans and V. Stevens, "NASA Engineering Models of the Mars Atmosphere for Entry Vehicle Design, "NASA TN-D-2525, November 1964.

5. Levenberg, K., "A Method for the Solution of Certain Non-linear Problems in Least Squares", Qu. Appl. Math., 2, 164-8, (1944).

6. Hartley, H.O., "The Modified Gauss-Newton Method for the Fitting of Non-linear Regression Functions by Least Squares," "Technometrics, 3, No. 2, May 1961.

7. "Space Probe Radar Altimeter Study", Texas Instruments Inc. Final Report, NASA CR-66383.

8. "Space Probe Radar Altimeter Study", Westinghouse Electric Corp. Final Report, NASA CR-66-262.

9. "Mars Probe/Lander Density Sensing System", Giannini Controls Corp. Final Report, NASA CR-66094.

10. Cefola, P.J., "Sensitivity Guidance for Entry into an Uncertain Martian Atmosphere", Ph.D. Thesis, Rensselaer Polytechnic Institute, November 1968.

11. Voyager Program, remarks by E.M. Cortright, NASA, presented at the Vth Annual Goddard Symposium, Voyage to the Planets Meeting, Washington, D.C., March 1967.

12. Brunelle, E.J., T.N. Kershaw, W.P. Rayfield and G.N. Sandor, "Landing on Mars by Autogyro", Rensselaer Review of Graduate Studies, No. 53, p. 19-23, October 1968.

13. Jenkins, [illegible] "A Numerical Method for Studying Transient Blade Motions of a Rotor with Flapping and Lead-Lag Degrees of Freedom," NASA TN-D-4195, October 1967.

14. United States Geological Survey Map, Nassau, N.Y., 1953, AMS 6269 II SE-Series V821, scale 1:24,000.

15. Preliminary Draft of Report on the Surface of Mars, Jet Propulsion Laboratory.

16. Miller, C., "Principles of Photographic Reproduction", New York, New York, (1942).

17. Sliva, T.F., "Chromatographic System Analysis: First-Order Model Evaluation", R.P.I. Technical Report MP-1, Sept. 1968, also Master's Project Report, Rensselaer Polytechnic Institute, Troy, N.Y. (1968).

18. Dankwerts, P.V., "Continuous Flow Systems", Chem. Eng. Sci., 2, 1 (1953).

19. Wehner, F.F., and Wilhelm, R.H., "Boundary Conditions of Flow Reactors", Chem. Eng. Sci., 6, 89 (1956).

20. Bastian, W.C., and Lapidus, L., "Longitudinal Diffusion in Ion Exchange and Chromatographic Columns. Finite Column", J. Phys. Chem., 60, 816 (1956).

21. Kucera, E., "Contribution to the Theory of Chromatography: Linear Non-Equilibrium Elution Chromatography", J. Chromatography, 19, 237 (1965).

22. Grubner, O., "Statistical Moments Theory of Gas-Solid Chromatography: Diffusion Controlled Kinetics," Advances in Chromatography, 6, 173 (1968).

23. Grubner, O., et.al., "Statistical Moments Theory of Gas-Solid Chromatography: Diffusion Controlled Kinetics," J. Chromatography, 28, 209 (1967).

24. Yamazaki, H., "A Mathematical Treatment of Non-Equilibrium Chromatography", J. Chromatography, 28, 14 (1967).

25. Wilhelm, R.H., "Progress Towards the A Priori Design of Chemical Reactors", Pure App. Chem., 5, 403 (1962).

26. Bischoff, K.B., "Mixing and Contacting in Chemical Reactors",

Ind. Eng. Chem., 58, 21 (Nov. 1966).

27. Hiby, J.W., "Process Symposium: Interaction of Fluids and Solids", Inst. Chem. Eng. (London), 312 (1962).

28. Bischoff, K.B., and Levenspiel, O., "Patterns of Flow in Chemical Process Vessels," Advance in Chem. Eng., 4, 95 (1963).

29. Taylor, G.I., "Dispersion of Soluble Matter in a Solvent Flowing Slowly Through a Tube," Proc. Royal Soc. (London), A219, 186 (1953).

30. Johnson, G., "Axial Dispersion from Flow Non-Uniformities in Packed Beds," Ph.D. Dissertation, Rensselaer Polytechnic Institute, Troy, New York (1967).

31. Rhodes, R., "Flow of Air in Beds of Spheres: A Statistical and Theoretical Approach", Ph.D. Dissertation, Rensselaer Polytechnic Institute, Troy, New York (1963).

32. Dorweiler, V.P., and Fahein, R.W., "Mass Transfer at Low Flow Rates in a Packed Column," AIChE J. 5, 139 (1959).